J. Am. Chem. Soc. 1986, 108, 40–56

C–H Activation Mechanisms and Regioselectivity in the Cyclometalation Reactions of Bis(pentamethylcyclopentadienyl)thorium Dialkyl Complexes

**Joseph W. Bruno,[†,‡] Gregory M. Smith,[†] Tobin J. Marks,*[†] C. Kay Fair,[§]
Arthur J. Schultz,*[⊥] and Jack M. Williams[⊥]**

*Contribution from the Department of Chemistry, Northwestern University,
Evanston, Illinois 60201, the Research Reactor, University of Missouri, Columbia,
Missouri 62511, and the Chemistry and Materials Science and Technology Divisions,
Argonne National Laboratory, Argonne, Illinois 60439.* *Received April 15, 1985*

Abstract: This contribution reports on the syntheses, structures, and cyclometalation reactions of a series of bis(pentamethylcyclopentadienyl)thorium dialkyl complexes of the type Cp'_2ThR_2 ($Cp' = \eta^5\text{-}C_5Me_5$). Thermal cyclometalation of $Cp'_2Th(CH_2CMe_3)_2$ proceeds unimolecularly in saturated hydrocarbon solvents to form the thoracyclobutane $Cp'_2Th(CH_2CMe_2CH_2)$ and CMe_4 with $\Delta H^{\ddagger} = 21.2\ (8)$ kcal mol^{-1} and $\Delta S^{\ddagger} = -16\ (2)$ eu. The molecular structure of $Cp'_2Th(CH_2CMe_3)_2$ has been determined by single-crystal neutron-diffraction techniques. This compound crystallizes in space group $P2_1/n$ with $a = 11.206\ (4)$ Å, $b = 16.670\ (6)$ Å, $c = 15.742\ (5)$ Å, $\beta = 93.48\ (2)°$, and $V = 2935\ (3)$ Å^3. The molecule exhibits a typical Cp'_2ThX_2 bent metallocene structure with highly unsymmetrical bonding of the neopentyl ligands, Th–C(α) = 2.543 (4) and 2.456 (4) Å; Th–C(α)–C(β) = 132.1 (3)°, and 158.2 (3)°. Consequences of these distortions include the acute angles Th–C(α)–H(α) = 84.4 (5)° and 87.1 (5)° in the ligand with Th–C(α)–C(β) = 158.2 (3)°. These distortions are proposed to reflect the severe steric congestion around the metal ion. Cyclometalation of $Cp'_2Th(CH_2SiMe_3)_2$ proceeds unimolecularly in either saturated or aromatic hydrocarbon solvents to yield $Cp'_2Th(CH_2SiMe_2CH_2)$ and $SiMe_4$ with $\Delta H^{\ddagger} = 25.1\ (4)$ kcal mol^{-1} and $\Delta S^{\ddagger} = -10.4\ (12)$ eu. Cyclometalation of $Cp'_2Th(CH_2CMe_3)(CH_2SiMe_3)$ proceeds unimolecularly in saturated and aromatic hydrocarbon solvents to form exclusively $Cp'_2Th(CH_2SiMe_2CH_2)$ and CMe_4 with $\Delta H^{\ddagger} = 19.4\ (2)$ kcal mol^{-1} and $\Delta S^{\ddagger} = -20.8\ (5)$ eu. This compound also displays a distorted dialkyl ligand geometry, with Th–C(α) = 2.44 (3) and 2.47 (3) Å and Th–C(α)–C(β) = 132 (3)° and Th–C(α)–Si = 150 (3)°. Cyclometalation of $Cp'_2Th(CH_2CMe_2Et)_2$ proceeds unimolecularly in saturated hydrocarbon solvents to form exclusively thoracyclobutane $Cp'_2Th(CH_2CMeEtCH_2)$ and CMe_3Et with $\Delta H^{\ddagger} = 18.5\ (7)$ kcal mol^{-1} and $\Delta S^{\ddagger} = -24\ (2)$ eu. Cyclometalation of $Cp'_2Th(CH_2SiMe_2Ph)_2$ proceeds unimolecularly in saturated or aromatic hydrocarbon solvents to form exclusively $Cp'_2Th(CH_2SiMePhCH_2)$ and $SiMe_3Ph$ with $\Delta H^{\ddagger} = 21.4\ (8)$ kcal mol^{-1} and $\Delta S^{\ddagger} = -20\ (2)$ eu. Upon further thermolysis, $Cp'_2Th(CH_2SiMePhCH_2)$ undergoes smooth conversion to $Cp'_2Th(CH_2SiMe_2\text{-}o\text{-}C_6H_4)$. Thermolysis of $Cp'_2Th(CHDSiMe_3)_2$ leads to formation of $(CH_2D)SiMe_3$, and thermolysis of $Cp'_2Th(CD_2CMe_3)_2$ leads to formation of $(CHD_2)CMe_3$, ruling out mechanisms involving significant α-hydrogen atom abstraction. Thermolysis of $Cp'_2Th[CH_2Si(CD_3)_3]_2$ leads to formation of both $(CH_2D)Si(CD_3)_3$ (process I, ~65%) and $(CH_3)Si(CD_3)_3$ (process II, ~35%). Process I, which proceeds with $\Delta H^{\ddagger} = 25.4\ (13)$ kcal mol^{-1} and $\Delta S^{\ddagger} = -14\ (4)$ eu, is attributed to the normal γ-hydrogen activating cyclometalation mechanism, while process II, with $\Delta H^{\ddagger} = 28.5\ (11)$ kcal mol^{-1} and $\Delta S^{\ddagger} = -3\ (3)$ eu, is attributed to a secondary mechanism involving rate-limiting abstraction of a hydrogen atom from a Cp′ ring, followed by hydrogen (deuterium) atom transfer from the remaining alkyl ligand to an intermediate $\eta^6\text{-}(CH_3)_4C_5CH_2$ species. Process I exhibits a large deuterium kinetic isotope effect, $k_H/k_D = 10.0\ (5)$ at 85 °C and $k_H/k_D = 8.5\ (6)$ at 115 °C. Solution and solid state CP–MAS ^{13}C NMR data are reported for the dialkyl complexes and are consistent with the structural data. The mechanism for cyclometalation is proposed to involve a concerted, heterolytic process with hydrogen atom abstraction and metallacycle formation occurring in a four-center transition state. Steric factors in the proposed transition state lead to discrimination between methyl and larger substituents on the β-carbon atom, accounting for the high observed regioselectivity. Steric factors also appear to impede intermolecular C–H activation processes involving solvent molecules.

The scope and mechanisms of homogeneous metal-centered processes in which C–H bond cleavage on a saturated hydrocarbon ligand is accompanied by metal–carbon bond formation (cyclometalation, e.g., eq 1) have been the subject of considerable current

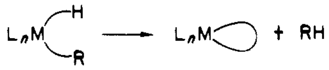

(1)

interest.[1-5] Such processes represent an important subset of transformations effecting homogeneous C–H bond activation[6,7] and because of their intramolecular nature[8] are frequently more facile and some of the most amenable to characterization. Furthermore, the metallacyclic[2,9] products of these reactions are of interest in their own right as demonstrated or proposed agents of olefin metathesis[10] and oligomerization,[11] C–H bond activation,[12] and hydrocarbon isomerization.[13]

Scheme I. Cyclometalation Mechanism Proposed for Bis(phosphine)platinum Dialkyl Complexes

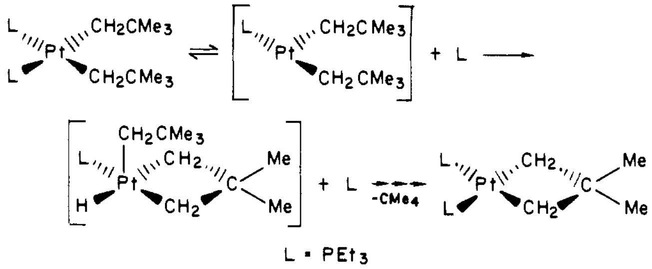

[†] Northwestern University.
[‡] Present address: Department of Chemistry, Wesleyan University, Middletown, CT 06457.
[§] University of Missouri.
[⊥] Argonne National Laboratory.

(1) For the purposes of this contribution, saturated hydrocarbon will refer to C–H bonds not immediately adjacent to heteroatoms (excluding silicon) or unsaturation.

0002-7863/86/1508-0040$01.50/0

With regard to mechanism, cyclometalation processes appear to fall into two general categories. Reaction sequences involving formal oxidative-addition[6d,e] of a C–H bond to the metal center, frequently followed by reductive-elimination of another fragment, are characteristic of electron-rich middle and late (e.g., platinum) transition metals. With regard to chemical, structural, and mechanistic systematics, these systems have received the greatest attention by far. A particularly well-characterized example is the bis(phosphine)platinum dialkyl series as illustrated by the $Pt(PEt_3)_2(CH_2CMe_3)_2$ cyclometalation mechanism of Scheme I.[3]

In contrast, cyclometalation chemistry involving early transition metals[2a] and f-element centers[4g,i,14] has not been extensively studied and is not well-characterized mechanistically. Such metal centers are frequently in relatively high (≥3) formal oxidation states, may not possess energetically accessible oxidation states for oxidative-addition/reductive-elimination sequences, and may be engaged in relatively polar metal–ligand bonding with "hard" rather than "soft" ligands. A particularly intriguing example of this type of cyclometalation process, which is superficially analogous to the transformation occurring in Scheme I, is the recently reported case of a Th(IV)-centered bis(neopentyl) → metallacyclobutane transformation (eq 2), $Cp' = \eta^5\text{-}(CH_3)_5C_5$).[14] Complete ligand dissociation as well as oxidative-addition/reductive-elimination processes appear unlikely here, and it is known that cyclometalation of the structurally distorted precursor molecules must overcome significant ring strain in the thoracyclobutane products[15] (which, in turn, can activate aromatic and some aliphatic hydrocarbon molecules when X = C[12,14]). The pathways by which such processes occur are the topic of this contribution.[16] We present here a detailed synthetic/mechanistic/structural discussion of our Cp'_2ThR_2 cyclometalation studies, focusing upon the pathway of C–H → C′–H hydrogen atom transfer, hydrogen atom positions in the ground state of $Cp'_2Th(CH_2CMe_3)_2$ by single-crystal neutron diffraction, and those structural/electronic factors influencing reaction rate and regioselectivity in both neopentyl and modified neopentyl complexes. While on the surface the present d^0,f^0 reaction patterns may appear to exhibit similarities to those of the d^8 and related systems, it will be seen that there are actually profound mechanistic differences. It will also be seen that Th–C bond enthalpy data are useful in understanding certain of the reaction patterns.

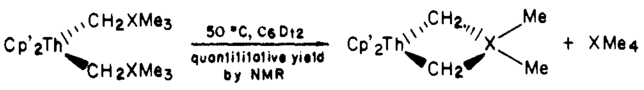

(2)

X = C, Si

Experimental Section

General Methods. All manipulations were carried out by using standard air free methodology in a nitrogen-filled Vacuum Atmospheres glovebox, on a Schlenk line, or in Schlenk-type apparatus interfaced to a high vacuum line. Solvents were purified and dried according to standard procedures. Cyclohexane-d_{12} (99.7% D) was obtained from Cambridge Isotopes Laboratories, Cambridge, MA, and was degassed and dried over NaK alloy prior to use. Lithium aluminum deuteride (99% D) was obtained from Norell Chemical Co., Inc., Landisville, NJ, and was used as received. Heavy water (99.8% D) was obtained from BIO-RAD Laboratory, Richmond, CA, and used after degassing, without further purification. Iodomethane-d_3 (99+ atom %, Gold Label), was obtained from Aldrich and dried over 4A molecular sieves prior to use. It could be converted to CD_3MgI in the usual manner in 96% yield.[17] Neopentyl chloride was obtained from Fairfield Chemical Co., Blythewood, SC, while (trimethylsilyl)methyl chloride and phenyl(dimethylsilyl)methyl chloride were obtained from Petrarch Systems, Inc., Bristol, PA. Neopentyllithium and (trimethylsilyl)methyllithium were prepared according to standard procedures. Pentamethylcyclopentadiene,[18] Cp'_2ThCl_2, and $Cp'_2Th(CH_2SiMe_3)Cl$ were prepared according to our published procedures.[19] Neohexyl bromide was kindly provided by Dr. Thom Tulip of E. I. du Pont de Nemours & Co., Inc., and was used after

---

(2) (a) Rothwell, I. P. *Polyhedron* **1985**, *4*, 177–200. (b) Collman, J. P.; Hegedus, L. S. "Principles and Applications of Organotransition Metal Chemistry"; University Science Books: Mill Valley, CA, 1980; pp 211–228.

(3) (a) Whitesides, G. M.; Reamey, R. H.; Brainard, R. L.; Izumi, A. N.; McCarthy, T. J. *Ann. N.Y. Acad. Sci.* **1983**, *415*, 56–66. (b) DiCosimo, R.; Moore, S. S.; Sowinski, A. F.; Whitesides, G. M. *J. Am. Chem. Soc.* **1982**, *104*, 124–133. (c) Ibers, J. A.; DiCosimo, R.; Whitesides, G. M. *Organometallics* **1982**, *1*, 13–20. (d) Whitesides, G. M. *Pure Appl. Chem.* **1981**, *53*, 287–292. (e) Foley, P.; DiCosimo, R.; Whitesides, G. M. *J. Am. Chem. Soc.* **1980**, *102*, 6713–6725. (f) Foley, P.; Whitesides, G. M. *J. Am. Chem. Soc.* **1979**, *101*, 2372–2373.

(4) (a) Calabrese, J. C.; Colton, M. C.; Herskovitz, T.; Klabunde, U.; Parshall, G. W.; Thorn, D. L.; Tulip, T. H. *Ann. N.Y. Acad. Sci.* **1983**, *415*, 302–313. (b) Tulip, T. H.; Thorn, D. L. *J. Am. Chem. Soc.* **1981**, *103*, 2448–2450. (c) Fuchita, Y.; Katsuma, H.; Uchiyama, T. *J. Chem. Soc., Dalton Trans.* **1983**, 897–899. (d) Shaw, B. L. *Adv. Chem. Ser.* **1982**, *196*, 101–115 and references therein. (e) Chamberlain, L.; Keddington, J.; Huffman, J. C.; Rothwell, I. P. *Organometallics* **1982**, *1*, 1538–1540. (f) Simpson, S. J.; Andersen, R. A. *Inorg. Chem.* **1981**, *20*, 3627–3629. (g) Simpson, S. J.; Turner, H. W.; Andersen, R. A. *Inorg. Chem.* **1981**, *20*, 2991–2995. (h) Clark, H. C.; Goel, A. B.; Goel, S. *Inorg. Chem.* **1979**, *18*, 2803–2808. (i) Simpson, S. J.; Turner, H. W.; Andersen, R. A. *J. Am. Chem. Soc.* **1979**, *101*, 7728–7729. (j) Andersen, R. A.; Jones, R. A.; Wilkinson, G. *J. Chem. Soc., Dalton Trans.* **1978**, 446–453. (k) Kiffen, A. A.; Masters, C.; Raynard, L. *J. Chem. Soc., Dalton Trans.* **1975**, 853–857. (l) Kletzin, H.; Werner, H. *Angew. Chem., Int. Ed. Engl.* **1983**, *22*, 873–874.

(5) For reviews dealing with related "ortho metalation" processes involving aromatic C–H bonds, see: (a) Constable, E. C. *Polyhedron* **1984**, *3*, 1037–1057. (b) Shilov, A. E. *Pure Appl. Chem.* **1978**, *50*, 725–733. (c) Bruce, M. I. *Angew. Chem., Int. Ed. Engl.* **1977**, *16*, 73–86.

(6) (a) Shilov, A. E. "Activation of Saturated Hydrocarbons by Transition Metal Complexes"; D. Reidel Publishers: Hingham, MA, 1984. (b) Reference 2b, pp 212–229. (c) Parshall, G. W. *Accts. Chem. Res.* **1975**, *8*, 113–117. (d) For theoretical work on C–H activation via oxidative addition and an illuminating discussion of what oxidative addition[6e] actually means in such circumstances, see: Saillard, J.-Y.; Hoffmann, R. *J. Am. Chem. Soc.* **1984**, *106*, 2006–2026 and references therein. (e) Crabtree, R. H.; Hlatky, G. *Inorg. Chem.* **1980**, *19*, 572–574.

(7) (a) Halpern, J. *Inorg. Chim. Acta* **1985**, *100*, 41–48. (b) Bergman, R. G. *Science* **1984**, *223*, 902–908. (c) Janowicz, A. H.; Kovac, C. A.; Periana-Pillia, R. A.; Buchanan, J. M.; Gilbert, T. M.; Bergman, R. G. "Organometallic Compounds. Synthesis, Structure, and Theory"; Shapiro, B. L., Ed.; Texas A&M University Press: College Station, TX, 1983; pp 420–452 and references therein. (d) Crabtree, R. H. *Ibid.*, pp 453–463 and references therein. (e) Jones, W. D.; Feher, F. J. *J. Am. Chem. Soc.* **1985**, *107*, 620–631 and references therein. (f) Hoyano, G. J.; McMaster, A. D.; Graham, W. A. G. *J. Am. Chem. Soc.* **1983**, *105*, 7190–7191 and references therein. (g) Watson, P. L. *J. Am. Chem. Soc.* **1983**, *105*, 6491–6493 and references therein. (h) Thompson, M. E.; Bercaw, J. E. *Pure Appl. Chem.* **1984**, *56*, 1–11.

(8) For a discussion of the thermodynamic and kinetic advantages of intramolecular reactions over intermolecular analogues, see: (a) Page, M. I. In "The Chemistry of Enzyme Action"; Page, M. I., Ed.; Elsevier: New York, 1984; pp 1–54. (b) Kirby, A. J. *Adv. Phys. Org. Chem.* **1980**, *17*, 183–278. (c) Page, M. I.; Jencks, W. P. *Proc. Natl. Acad. Sci. U.S.A.* **1971**, *68*, 1678–1683.

(9) (a) Chappell, D. S.; Cole-Hamilton, S. D. *Polyhedron* **1982**, *1*, 739–777. (b) Puddephatt, R. J. *Comments Inorg. Chem.* **1982**, *2*, 69–95. (c) Puddephatt, R. J. *Coord. Chem. Rev.* **1980**, *33*, 149–183. (d) Puddephatt, R. J. *ACS Symp. Ser.* **1983**, *211*, 353–367.

(10) (a) Rocklage, S. M.; Fellman, J. D.; Rupprecht, G. A.; Messerle, L. W.; Schrock, R. R. *J. Am. Chem. Soc.* **1981**, *103*, 1440–1447. (b) Lee, J. B.; Howard, T. R.; Grubbs, R. H. *J. Am. Chem. Soc.* **1980**, *102*, 6876–6878. (c) Wengrovius, J. H.; Schrock, R. R.; Churchill, M. R.; Missert, J. R.; Youngs, W. J. *J. Am. Chem. Soc.* **1980**, *102*, 4515–4516. (d) Grubbs, R. H. *Prog. Inorg. Chem.* **1978**, *24*, 1–50. (e) Katz, T. J. *Adv. Organomet. Chem.* **1977**, *16*, 282–317.

(11) Irvin, K. J.; Rooney, J. J.; Stewart, C. D.; Green, M. L. H.; Mantab, R. *J. Chem. Soc., Chem. Commun.* **1978**, 604–606.

(12) (a) Fendrick, C. M.; Marks, T. J. *J. Am. Chem. Soc.* **1984**, *106*, 2214–2216. (b) Fendrick, C. M.; Marks, T. J. *J. Am. Chem. Soc.*, in press.

(13) (a) O'Donohoe, C.; Clarke, J. K. A.; Rooney, J. J. *J. Chem. Soc., Chem. Commun.* **1979**, 648–649. (b) O'Donohoe, C.; Clarke, J. K. A.; Rooney, J. J. *J. Chem. Soc., Faraday Trans. 1* **1980**, *76*, 345–356. (c) Hugues, R.; Besson, B.; Basset, J. M. *J. Chem. Soc., Chem. Commun.* **1980**, 719–721. (d) Clarke, J. K. A.; Rooney, J. J. *Adv. Catal.* **1976**, *25*, 125–183.

(14) (a) Bruno, J. W.; Marks, T. J.; Day, V. W. *J. Am. Chem. Soc.* **1982**, *104*, 7357–7360. (b) Bruno, J. W.; Marks, T. J.; Day, V. W. *J. Organomet. Chem.* **1983**, *250*, 237–246.

(15) Bruno, J. W.; Marks, T. J.; Morse, L. R. *J. Am. Chem. Soc.* **1983**, *105*, 6824–6832.

(16) For a preliminary account of some of this work, see: Bruno, J. W.; Duttera, M. R.; Fendrick, C. M.; Smith, G. M.; Marks, T. J. *Inorg. Chim. Acta* **1984**, *94*, 271–277.

(17) Determined by acid–base titrations of clear aliquots of the reaction mixture after the reaction had been filtered through Celite and concentrated slightly.

(18) Mintz, E. A.; Schertz, L. D.; Marks, T. J., manuscript in preparation.

(19) Fagan, P. J.; Manriquez, J. M.; Maatta, E. A.; Seyam, A. M.; Marks, T. J. *J. Am. Chem. Soc.* **1981**, *103*, 6650–6667.

drying over P_2O_5. Known compounds $Cp'_2Th(CH_2CMe_3)_2$ (**1**), $Cp'_2Th(CH_2SiMe_3)_2$ (**3**), and the deuterated alkyls $Cp'_2Th(CHDSiMe_3)_2$ (**11**), $Cp'_2Th(CD_2CMe_3)_2$ (**12**), and $Cp'_2Th[CH_2Si(CD_3)_3]_2$ (**13**) were prepared according to the literature procedures,[19] with deuterated reagents substituted where necessary.

Proton NMR spectra were recorded at 90 MHz on a Varian Model EM-390 or at 270 MHz on a JEOL Model FX-270 instrument. Carbon NMR spectra were recorded at 67.80 MHz on a JEOL Model FX-270 instrument, and solid-state ^{13}C CP-MAS NMR spectra were recorded at 15.00 MHz on a JEOL Model FX60QS. GLC traces were obtained on a Varian Model 3700 gas chromatograph equipped with FID detection and a Hewlett-Packard 3390A digital recorder/integrator, using a 0.125 in. i.d. column with 3.8% w/w SE-30 liquid phase on Chromosorb G support. GC–MS measurements were made on a Hewlett-Packard Model 5985A GC/MS system with electron impact ionization at 15 eV unless otherwise noted. An SE-30 column was also utilized in this instrument. Elemental analyses were carried out by Dornis und Kolbe Mikroanalytisches Laboratories, Mülheim/Ruhr, West Germany.

$Cp'_2Th(CH_2CMe_2CH_2)$ (2). In the glovebox, 1.5 g (2.3 mol) of **1** was placed in a 100-mL flask which was then attached to a frit apparatus. On the vacuum line, heptane (50 mL) was condensed into the flask. An argon atmosphere was admitted to the flask and the solution stirred for 60 h while immersed in a 50 °C oil bath. After the mixture was cooled, the volatiles were pumped off and collected in a liquid nitrogen cooled trap for subsequent analysis by GC–MS. In addition to the heptane solvent, the volatiles contained neopentane. The orange residue from the reaction was then taken up in heptane (ca. 15 mL) and filtered to remove a small amount of insoluble orange material. The filtrate was cooled to −78 °C to precipitate the yellow product, which was collected by cold filtration and washed several times with condensed heptane to remove traces of an oily orange impurity. The compound was then dried in vacuo to give 0.87 g of **2** (65%).

^1H NMR (C_6D_{12}): δ 1.98 (s, 30 H, $(CH_3)_5C_5$), 1.29 (s, 6 H, $C(CH_3)_2$), 0.92 (s, 4 H, $Th(CH_2)_2C$). ^{13}C NMR (C_6D_{12}): δ 123.3 (s, C_5Me_5), 94.0 (t, J_{CH} = 123 Hz, $ThCH_2C$), 39.4 (q, J_{CH} = 123 Hz, $C(CH_3)_2$), 15.8 (s, $C(CH_3)_2$), 11.7 (q, J_{CH} = 126 Hz, $(CH_3)_5C_5$).

Anal. Calcd for $C_{25}H_{40}Th$: C, 52.34; H, 7.04. Found: C, 51.96; H, 6.86.

In a separate experiment, ca. 30 mg of **2** was dissolved in 5 mL of heptane and hydrolyzed with D_2O. The volatiles were collected and analyzed by GC–MS which identified, in addition to heptane, Cp′D (*m/e* 137) and $Me_2C(CH_2D)_2$ (*m/e* 58, 57).

$Cp'_2Th(CH_2SiMe_2CH_2)$ (4). In the glovebox, a 100-mL flask was charged with 1.60 g (2.4 mmol) of **3** and attached to a frit apparatus. On the vacuum line, heptane (ca. 40 mL) was condensed into the flask and an argon atmosphere provided. The flask was immersed in an 85 °C oil bath and stirred at this temperature for 36 h. After this period, the volatiles were removed and collected in a trap at 77 K for subsequent analysis by GC–MS. In addition to heptane, the volatiles contained Me_4Si. The yellow residue from the reaction was taken up in heptane (20 mL), filtered, and cooled to −78 °C to precipitate the yellow, microcrystalline product. Cold filtration afforded 1.04 g of **4** (75%).

^1H NMR (C_6D_{12}): δ 1.98 (s, 30 H, $(CH_3)_5C_5$), 0.43 (s, 4 H, $Th(CH_2)_2Si$), 0.22 (s, 6 H, $Si(CH_3)_2$). ^{13}C NMR (C_6D_{12}): δ 123.2 (s, C_5Me_5), 69.0 (t, J_{CH} = 120 Hz, $ThCH_2Si$), 11.7 (q, J_{CH} = 126 Hz, $(CH_3)_5C_5$), 2.4 (q, $SiCH_3$).

Anal. Calcd for $C_{24}H_{40}SiTh$: C, 48.96; H, 6.85. Found: C, 48.69; H, 6.96.

In a separate experiment, ca. 30 mg of **4** was dissolved in 5 mL of heptane and hydrolyzed with D_2O. The volatiles were collected and analyzed by GC–MS. Present, in addition to heptane, were Cp′D (*m/e* 137) and $Me_2Si(CH_2D)_2$ (*m/e* 90, 75, 74).

$Cp'_2Th(CH_2CMe_3)(CH_2SiMe_3)$ (5). In the glovebox, a 50-mL round-bottomed flask was charged with 1.95 g (3.1 mmol) of $Cp'_2Th(CH_2SiMe_3)Cl$ and 0.25 g (3.2 mmol) of $LiCH_2CMe_3$ and connected to a frit apparatus. It is imperative that the $Cp'_2Th(CH_2SiMe_3)Cl$ used be free of **3** before reaction as **3** and **5** cannot be separated by fractional crystallization. On the vacuum line, diethyl ether (25 mL) was condensed into the flask at −78 °C resulting in a cloudy, colorless mixture. After being stirred at −78 °C for 10 min, the mixture was immersed in an ice bath and stirred for ca. 4 h. After this time, significant amounts of white solid had formed in the reaction mixture. The ether was next removed in vacuo at 0 °C and the residue extracted with 25 mL of heptane and filtered. The insoluble materials were washed once by condensing ca. 10 mL of the heptane into the upper part of the frit apparatus. The washings were combined with the filtrate, and the resulting clear, colorless solution was concentrated and cooled to −78 °C. After the solution was left to stand overnight, filtration at −78 °C afforded 1.41 g (68%) of analytically pure **5** as fine, colorless crystals.

^1H NMR (C_6D_6): δ 2.00 (s, 30 H, $(CH_3)_5C_5$), 1.24 (s, 9 H, $C(CH_3)_3$), 0.34 (s, 9 H, $Si(CH_3)_3$), 0.02 (s, 2 H, $ThCH_2C$), −0.44 (s, 2 H, $ThCH_2Si$). ^1H NMR (C_6D_{12}): δ 2.10 (s, 30 H, $(CH_3)_5C_5$), 1.04 (s, 9 H, $C(CH_3)_3$), 0.08 (s, 9 H, $Si(CH_3)_3$), −0.08 (s, 2 H, $ThCH_2C$), −0.58 (s, 2 H, $ThCH_2Si$).

Anal. Calcd for $C_{29}H_{52}SiTh$: C, 52.71; H, 7.93. Found: C, 51.93; H, 7.85.

Thermolysis of 5. In the glovebox, ca. 60 mg of **5** was loaded into a clean dry NMR tube which was then fitted into a 5-mm O-ring vacuum adaptor and interfaced to the high-vacuum line. On the vacuum line, C_6D_{12} (ca. 0.4 mL) from a reservoir also containing NaK alloy was condensed into the tube. The solvent was frozen at −78 °C and the NMR tube sealed off in vacuo. The sample was then warmed to room temperature and dissolved, and the 90-MHz ^1H NMR spectrum was recorded to verify the purity of the sample. The tube was then immersed in an 85 °C thermostated oil bath for 3 h and the ^1H NMR spectrum recorded again. It was identical with a spectrum of authentic **4** prepared from **2**. Identical results were obtained when C_6D_6 was used as a solvent.

$Cp'_2Th(CH_2CMe_2Et)_2$ (6). Neohexyllithium was synthesized in 50% titrated yield[17] as a pentane solution by metalating dry neohexyl bromide with lithium sand (1% Na) at room temperature for 1 week (vide infra). For complex **6**, a pentane solution (ca. 50 mL) containing 14.1 mmol of lithium reagent was transferred under argon via syringe into a two-necked 100-mL round-bottomed flask connected to a frit apparatus. After removal of solvent in vacuo, a waxy white solid was obtained. The apparatus was brought into the glovebox and a bent solid addition tube attached to the second neck of the flask and charged with 3.80 (6.7 mmol) Cp'_2ThCl_2. On the vacuum line, ether (50 mL) was condensed into the flask at −78 °C and the resulting solution allowed to stir and equilibrate with the temperature of the bath. The Cp'_2ThCl_2 was then added all at once by turning the addition tube and the white mixture was allowed to warm to 0 °C with stirring. As the mixture warmed, it first became nearly homogeneous and shortly thereafter became cloudy again. The mixture was allowed to stir at 0 °C overnight to ensure complete reaction before removing the ether in vacuo and condensing in pentane (20 mL). Filtration separated a pale yellow solution from some slightly colored solids. The solids were extracted with 2 × 10 mL of pentane by condensing the pentane into the upper part of the apparatus, and the pentane was removed in vacuo from the combined filtrate and washings. The residue was triturated with 5 mL of pentane and the solvent then removed in vacuo three times before finally condensing in just enough pentane to dissolve the residue at room temperature. The solution was cooled to −78 °C and after 2 days 2.0 g (75%) of colorless crystals were collected by cold filtration.

^1H NMR (C_6D_{12}): δ 2.09 (s, 30 H, $(CH_3)_5C_5$), 1.33 (q, 2 H, $^3J_{HH}$ = 7.5 Hz, CCH_2CH_3), 1.00 (s, 3 H, CCH_3), 0.86 (t, 3 H, $^3J_{HH}$ = 7.5 Hz, CH_2CH_3), −0.11 (s, 2 H, $ThCH_2$). ^1H NMR (C_6D_6): δ 2.04 (s, 30 H, $(CH_3)_5C_5$), 1.54 (q, 2 H, $^3J_{HH}$ = 7.5 Hz, CCH_2CH_3), 1.21 (s, 3 H, CCH_3), 1.06 (t, 3 H, $^3J_{HH}$ = 7.5 Hz, CH_2CH_3), 0.03 (s, 2 H, $ThCH_2$).

Anal. Calcd for $C_{32}H_{56}Th$: C, 57.12; H, 8.39. Found: C, 57.17, H, 8.12.

$Cp'_2Th(CH_2C(Me)(Et)CH_2)$ (7). A sample of **6** in C_6D_{12} was thermolyzed at 60 °C and the reaction monitored by ^1H NMR at 270 MHz. Figure S-1[20] shows typical spectra obtained from this thermolysis. The inequivalent Cp′ resonances and the presence of an ethyl resonance suggested clean formation of a 2-methyl-2-ethylthoracyclobutane. To confirm this, a 30-mL flask was charged in the glovebox with 2.90 g (4.3 mmol) of **6** and connected to a frit apparatus. On the vacuum line, cyclohexane (ca. 15 mL) was condensed into the flask to give a colorless solution which was then stirred while immersed in an 80 °C oil bath. Progress of the reaction was monitored by following the Cp′ resonances in a sealed NMR sample being thermolyzed concurrently. After ca. 3.5 half-lives, the orange solution was cooled to room temperature and filtered to remove a small amount of orange insoluble material. The cyclohexane was removed in vacuo and a small amount of pentane condensed into the flask, dissolving the product. Cooling this solution to −78 °C and agitating it precipitated yellow microcrystals of **7**. Isolation by cold filtration gave 1.73 g (68%) of **7** as a bright yellow solid. The assignment of the ^1H NMR spectra is discussed in the Results section.

^1H NMR (C_6D_{12}): δ 1.99 (s, 15 H, $(CH_3)_5C_5$ A), 1.96 (s, 15 H, $(CH_3)_5C_5$ B), 1.42 (q, 2 H, $^3J_{HH}$ = 7.2 Hz, CCH_2CH_3), 1.12 (s, 3 H, CCH_3), 0.95 (t, 3 H, $^3J_{HH}$ = 7.2 Hz, CCH_2CH_3), 0.89 (d, 2 H, $^2J_{HH}$ = 14 Hz, $ThCH_AH_BC$), 0.77 (d, 2 H, $^2J_{HH}$ = 14 Hz, $ThCH_AH_BC$). ^1H NMR (C_6D_6): δ 1.93 (s, 15 H, $(CH_3)_5C_5$ A), 1.91 (s, 15 H, $(CH_3)_5C_5$ B), 1.77 (q, 2 H, $^3J_{HH}$ = 7.2 Hz, CCH_2CH_3), 1.47 (s, 3 H, CCH_3), 1.30 (t, 3 H, $^3J_{HH}$ = 7.2 Hz, CCH_2CH_3), 1.17 (d, 2 H, $^2J_{HH}$ = 14 Hz, $ThCH_AH_BC$), 1.05 (d, 2 H, $^2J_{HH}$ = 14 Hz, $ThCH_AH_BC$).

---

(20) See paragraph at end of paper regarding supplementary material.

Anal. Calcd for $C_{26}H_{42}Th$: C, 53.23; H, 7.22. Found: C, 53.17; H, 7.09.

Reaction of 7 with Me_4Si. As a further test of the formulation of 7 as a thoracyclobutane, the reaction of 7 with Me_4Si was studied by ^1H NMR. A sample of 7 was dissolved in C_6D_{12} containing Me_4Si to give a yellow solution. This solution was freeze–pump–thaw degassed and the tube sealed in vacuo. Reaction was complete, as judged by ^1H NMR, within 1 h to give a decolorized solution with a spectrum (Figure S-2)[20] consistent with the expected ring-opened product.

$LiCH_2SiMe_2Ph$. Before being used in this reaction, $ClCH_2SiMe_2Ph$ was thoroughly dried by stirring for several days over P_2O_5 followed by distillation under argon. Immediately before use, sufficient Li (50% dispersion in mineral oil) to ensure stoichiometric excess in the following reaction was mixed with dry pentane, the resulting mixture filtered, and the lithium sand washed several times with pentane to remove residual oil. After being dried in vacuo, the sand was brought into the glovebox and transferred to a 100-mL flask equipped with a gas inlet. On a Schlenk line, the atmosphere in the flask was changed from N_2 to Ar, and pentane (50 mL) was added to the flask under flush. Next, with use of a tared syringe, 7.8 g (42 mmol) of $ClCH_2SiMe_2Ph$ was delivered under an Ar flush to the flask. A reflux condenser was connected to the flask and the gray reaction mixture refluxed for 1 week. After this time, the reaction was cooled and the purple mixture filtered through Celite. The gray and purple insoluble matter was then washed with pentane (7 × 20 mL) and the clear colorless combined filtrate concentrated in vacuo, leading to formation of a large amount of colorless crystals. Filtration at room temperature gave 4.51 g (68%) of $LiCH_2SiMe_2Ph$.

^1H NMR (C_6D_6): δ −2.38 (s, 2 H, $LiCH_2$), 0.15 (s, 6 H, $Si(CH_3)_2$), 7.15–7.65 (m, 5 H, C_6H_5).

$Cp'_2Th(CH_2SiMe_2Ph)_2$ (8). In the glovebox, a 100-mL round-bottomed flask was charged with 4.50 g (7.80 mmol) of Cp'_2ThCl_2 and 2.47 g (15.8 mmol) of $LiCH_2SiMe_2Ph$. The flask was attached to a frit apparatus, removed from the glovebox, and connected to the vacuum line. The flask was next evacuated and diethyl ether (50 mL) condensed into the flask. An argon atmosphere was admitted to the flask, and the white mixture was stirred while it was allowed to warm to 0 °C. As the mixture warmed, some of the initial material dissolved, clearing the solution somewhat, until material began to reprecipitate from the solution. After the solution had stirred at 0 °C for ca. 5 h, the ether was removed in vacuo and the white residue twice triturated with a few mL of heptane and dried in vacuo. Extraction of this residue through the frit with pentane (50 mL), followed by 2 × 10 mL Soxhlet-type extraction of the insolubles, separated a clear colorless solution from the white insoluble material. The pentane solution was next concentrated in vacuo until a large quantity of colorless crystalline solid was present at room temperature. This mixture was cooled to −78 °C, an argon atmosphere admitted, and the mixture allowed to stand overnight. The next day, cold filtration separated a colorless crystalline powder from the clear, colorless supernatant. After drying in vacuo, 5.00 g (80%) of 8 was collected in the glovebox.

^1H NMR (C_6D_6): δ −0.26 (s, 4 H, $ThCH_2$), 0.57 (s, 12 H, $Si(CH_3)_2$), 1.84 (s, 30 H, $(CH_3)_5C_5$), 7.25–7.83 (m, 10 H, C_6H_5).

Anal. Calcd for $C_{38}H_{56}Si_2Th$: C, 56.98; H, 7.01. Found: C, 56.98; H, 6.95.

$Cp'_2\overline{Th(CH_2SiMePhCH_2})$ (9). A one-necked 30-mL round-bottomed flask was charged in the glovebox with 2.10 g (2.6 mmol) of 8 and connected to a frit apparatus. On the vacuum line, the flask was evacuated and heptane (15 mL) condensed in, dissolving 8. The flask was pressurized with ca. 1 atm of argon at room temperature and closed tightly. Meanwhile, an NMR sample of 8 was prepared in C_7D_8 in a sealed tube. Both the flask and the NMR tube were immersed in an oil bath at ca. 80 °C and the contents of the flask were stirred. The progress of the reaction was monitored via NMR, and after several days the reaction was stopped when most of the material had been converted to 9. It is important, however, to stop the reaction before completion so that formation of 10 is minimized. Since 10 is slightly less soluble than 8 it is not possible to remove large amounts (>5%) by recrystallization. The pale yellow solution was filtered while hot, allowed to cool to room temperature, concentrated, and cooled to −78 °C to crystallize the metallacycle. After the solution was allowed to stand overnight, cold filtration separated pale yellow crystals of 9 from the yellow supernate. After the solution was dried in vacuo 1.10 g (64%) of 9 was collected in the glovebox.

^1H NMR (C_6D_6): δ 0.68 (s, 3 H, $SiCH_3$), 0.87 (d, 2 H, $ThCH_AH_B$, $^2J_{HH}$ = 13.8 Hz), 1.03 (d, 2 H, $ThCH_AH_B$, $^2J_{HH}$ = 13.8 Hz), 1.76 (s, 15 H, $(CH_3)_5C_5$ A), 1.88 (s, 15 H, $(CH_3)_5C_5$ B), 8.10, 7.47–7.20 (m, 5 H, C_6H_5). ^{13}C NMR (C_6D_6): δ 3.00 (q, J_{CH} = 119 Hz, $SiCH_3$), 11.3 (q, J_{CH} = 125 Hz, $(CH_3)_5C_5$ A), 11.4 (q, J_{CH} = 125 Hz, $(CH_3)_5C_5$ B), 64.0 (t, J_{CH} = 120 Hz, $ThCH_2$), 123.2 (s, $(CH_3)_5C_5$ A), 123.5 (s, $(CH_2)_5C_5$ B), aryl carbon atoms were partially obscured by the solvent resonance, but could be located—127.7 (d, J_{CH} = 158 Hz), 128.5 (d, J_{CH} = 156 Hz), 136.2 (d, J_{CH} = 156 Hz), 143.4 (s).

Anal. Calcd for $C_{29}H_{42}SiTh$: C, 53.53; H, 6.51. Found: C, 53.60; H, 6.90.

$Cp'_2\overline{Th(CH_2SiMe_2\text{-}o\text{-}C}_6H_4)$ (10). Working in the glovebox, a 50-mL flask was charged with 1.65 g of 9 and connected to a frit apparatus. On the vacuum line, the flask was evacuated and heptane (25 mL) condensed into the flask to dissolve the 9, giving a clear, pale yellow solution. Argon (ca. 1 atm) was admitted to the flask and the apparatus closed tightly. Meanwhile, another sample of 9 was sealed off in an NMR tube with C_7D_8. Both the NMR tube and the reaction flask were immersed with stirring in a 100 °C oil bath. When NMR indicated that the reaction was essentially complete (ca. 1 week), the heater for the oil bath was turned off and the clear yellow solution allowed to cool slowly. After the solution was left to stand overnight, filtration separated pale yellow needles from the yellow mother liquor. This material was collected in the glovebox and allowed to dry in the box atmosphere; yield 0.46 g. A second crop of crystals was collected from the mother liquor by concentrating and cooling to −78 °C; combined yield: 1.24 g (75%).

^1H NMR (C_6D_6): δ 0.61 (s, 6 H, $SiCH_3$), 0.74 (s, 2 H, $ThCH_2$), 1.86 (s, 30 H, $(CH_3)_5C_5$), 7.67–7.19 (m, 4 H, C_6H_4). $^{13}C\{^1H\}$ NMR (C_6D_6): δ 4.5 ($SiCH_3$), 11.5 ($(CH_3)_5C_5$), 66.3 ($ThCH_2$), 124.0 ($(CH_3)_5C_5$); only 5 aryl peaks could be located—126.5, 127.0, 134.2, 134.4, 148.9.

Anal. Calcd for $C_{29}H_{42}SiTh$: C, 53.53; H, 6.51. Found: C, 53.63; H, 6.76.

$Cp'_2Th(CH_2CH_2CH_3)_2$. In an attempted synthesis of Cp'_2Th(isopropyl)$_2$, a frit apparatus was charged with 1.25 g (2.18 mmol) of Cp'_2ThCl_2. On the vacuum line, 15 mL of Et_2O was condensed in at −78 °C and, under an argon flush, 1.9 mL of 3.0 M *i*-PrMgBr in Et_2O was added by syringe. The mixture was stirred at −78 °C for 20 min and then allowed to warm to room temperature for 2 h. The solvent was removed in vacuo and 15 mL of heptane was condensed into the vessel. The mixture was then filtered, the solids washed with condensed heptane, and the combined solutions cooled to −78 °C. The colorless product was collected by filtration, washed with 5 mL of condensed solvent, and dried; yield 1.13 g (75%).

^1H NMR (C_6D_{12}): δ 0.013 (t, 4 H), 0.963 (t, 6 H), 1.256 (m, 4 H), 2.001 (s, 30 H).

The mechanism of this reaction probably involves β-hydride elimina-

---

(21) (a) Nystrum, R. F.; Brown, W. G. *J. Am. Chem. Soc.* **1947**, *69*, 1197–1199. (b) Riley, G. A.; Hershkowitz, R. L.; Rein, B. B.; Chung, B. C. *J. Am. Chem. Soc.* **1964**, *86*, 964–966.

(22) Burford, C.; Cooke, F.; Erliner, E.; Magnus, P. *J. Am. Chem. Soc.* **1977**, *99*, 4536–4537.

(23) Decker, O. W.; Post, H. W. *J. Org. Chem.* **1960**, *25*, 249–252.

(24) Observed mass spectra for isotopically substituted materials (*m/e*: rel int): Me_3CCD_2H (25 eV) 53:0.2, 54:0.2, 55:1.0, 56:2.7, 57:32.8, 58:6.2, 59:100, 60:4.4, 61:0.1; $Me_3Si(CDH_2)$ (70 eV) 69:0.1, 70:0.3, 71:0.6, 73:35.9, 74:100.0, 75:11.6, 76:4.0, 77:0.2, 89:1.9; $Me_4Si\text{-}d_9$ (15 eV) 77:0.2, 78:4.2, 79:100.0, 80:8.7, 81:6.1, 82:41.7, 83:3.6, 84:1.5; $Me_4Si\text{-}d_{10}$ (15 eV) 77:0.5, 78:0.2, 79:5.3, 80:100, 81:10.8, 82:41.7, 83:41.7, 83:3.4, 84:1.4; $Cp'H\text{-}d_0$ (15 eV, authentic sample) 105:9.8, 106:1.7, 107:3.0, 108:1.8, 109:0.2, 119:2.8, 120:0.5, 121:78.8, 122:7.9, 123:0.4, 135:2.9, 136:100.0, 137:11.5, 138:6.6; $Cp'H\text{-}d_1$ (calculated based on equal probability of loss of CH_3 groups) 105:3.9, 106:0.6, 107:2.2, 108:2.5, 109:1.2, 119:0.6, 120:1.5, 121:16.2, 122:64.6, 123:64.6, 124:0.3, 136:2.9, 137:100.0, 138:11.5, 139:6.6; $Me_4Si\text{-}d_1$ (90 eV, major peaks only) 70:0.3, 71:0.6, 73:35.9, 74:100, 75:11.6, 76:4.0, 77:0.2, 89:1.9, 90:0.2; neopentane-d_2 (25 eV, major peaks only) 40:1.8, 41:13.2, 43:9.4, 44:1.1, 55:1.0, 56:2.7, 57:32.8, 58:6.2, 59:100.0, 60:4.4, 61:0.1.

(25) Robinson, E. A. "Least Squares Regression Analysis in Terms of Linear Algebra"; Goose Pond Press: Houston, 1981.

(26) Observed mass spectra were modeled, after normalization, as a linear combination of the normalized spectra of $Me_4Si\text{-}d_9$ and $Me_4Si\text{-}d_{10}$ and a constant function, arbitrarily set to 1. In no case did the dummy contribution amount to more than 2% of the least-squares fit. Regression coefficients were calculated in the usual fashion, with standard deviations obtained from the variance–covariance matrix. All of the regression fits were highly significant at the 0.01 level in an *F*-test, with calculated *F* values which typically exceeded the critical values by at least an order of magnitude. Adjusted reduction ratios (*R* values) were all in the range 0.96–0.99.

(27) Bruno, J. W.; Marks, T. J.; Day, V. W., unpublished results.

(28) (a) Bacon, G. E. In "International Tables for X-ray Crystallography"; Kynoch Press: Birmingham, England, 1974; Vol. IV, pp 99–101. (b) Bacon, G. E. In *Ibid.*, p 270.

(29) Smith, G. M.; Marks, T. J.; Day, V. W., manuscript in preparation.

(30) Thoracyclobutanes containing three carbon atoms in the ring react with unhindered aryl C–H bonds to yield the corresponding bisaryl complexes.[12,14a]

(31) Berry, M.; Elmitt, K.; Green, M. L. H. *J. Chem. Soc., Dalton Trans.* **1979**, 1950–1958.

tion followed by readdition and is discussed elsewhere.[32]

Me_3CCD_2OH. In a modification of the literature procedure for the protio analogue,[21a] 11 mL (d = 0.979 g cm^{-3}, 89.3 mmol) of $Me_3CC(O)Cl$ in diethyl ether (10 mL) was added dropwise at a rate sufficient to maintain a gentle reflux to 2.0 g of $LiAlD_4$ (48 mmol, limiting reagent) in an ice cold, stirred, diethyl ether (40 mL) slurry. After being stirred overnight the reaction mixture was quenched with ice water (10 mL). Working in air, the reaction mixture was then poured into ice water (20 mL) and the resultant mixture poured into 10% aqueous H_2SO_4 (100 mL). The ether layer was separated from the aqueous phase and combined with 3 × 100 mL ether washings of the aqueous phase. The organic phase was dried overnight with $CaCl_2$ and concentrated on a rotary flash evaporator, and the residue was distilled to isolate 5.92 g of the alcohol (69% based on LAD, bp 113–115 °C, cf. lit. bp 113–114 °C for protio material). On the basis of MS data, the methylene is estimated to contain ≥99 atom % D.

Me_3CCD_2Br, Me_3CCD_2Li, and $Cp'_2Th(CD_2CMe_3)_2$. Neopentyl-*1,1'*-d_2 bromide was prepared by a modification of the literature procedure for the protio analogue.[21b] The alcohol Me_3CCD_2OH (5.92 g, 165.6 mmol), freshly distilled dry DMF (65 mL), and distilled Aldrich PBu_3 (19 mL, 76 mmol) were combined in a three-necked reaction flask. The reaction flask was lowered into a cold water bath and Br_2 (Dow Chemical Co.) was added dropwise until an orange solution was obtained. After stirring overnight, the reaction mixture was vacuum distilled to obtain a mixture of DMF and Me_3CCD_2Br. Water was added to this mixture until an organic layer separated, which was then collected. After a simple distillation from P_2O_5 to remove H_2O and the last traces of DMF, 5.41 g (41%) of Me_3CCD_2Br was obtained.

This material was subsequently lithiated and converted to $Cp'_2Th(CD_2CMe_3)_2$ in the usual manner (vide supra). It was found to be >98% CD_2 in the methylene positions by ^1H NMR and by hydrolysis, followed by GC–MS of the evolved neopentane. General procedures for analyzing the thermolysis products were the same as for $Cp'_2Th[CH_2Si(CD_3)_3]_2$ (vide infra).

$LiCHDSiMe_3$ and $Cp'_2Th(CHDSiMe_3)_2$. The precursor $Me_3SiCHDCl$ proved difficult to prepare, but sufficient material was obtained in the first preparation that a second synthesis was not attempted. In a slight modification of the literature procedure[22] for generating $LiCH(Cl)SiMe_3$, dry THF (80 mL) was combined with predried 4A molecular sieves and freshly distilled $ClCH_2SiMe_3$ (9.0 mL, 64 mmol) in a 500-mL three-necked flask. The resultant solution was cooled to −78 °C and stirred. *sec*-Butyllithium (47 mL, 1.5 M solution in cyclohexane, 71 mmol) was slowly added dropwise to the cold solution. After this addition was complete, TMEDA (10.2 mL, 67 mmol), freshly distilled from BaO, was also added in a dropwise fashion to the reaction mixture. The resulting mixture was stirred for 45 min and then removed from the cooling bath and allowed to warm slowly to −55 °C. At this point, D_2O (5 mL) was quickly syringed into the reaction while it was vigorously stirred. After the mixture was warmed to room temperature, the reaction was quenched by pouring it into an equal volume of saturated aqueous NH_4Cl. The organic phase was separated and combined with an additional hexane extract of the aqueous phase. An unknown amount of $Me_3SiCHDCl$ was obtained as a mixture with cyclohexane after an attempted distillation. This mixture was dried over $CaCl_2$ and metalated with Li sand (1% Na) in the usual manner to obtain, after filtration and evaporation of the cyclohexane, 70 mg of the lithium reagent (identified by ^1H NMR), with isotopic substitution estimated to be >98.5 atom % D. It was converted to $Cp'_2Th(CHDSiMe_3)_2$ in the usual manner (vide supra). ^1H NMR and hydrolysis followed by GC–MS showed this complex to be >98% monodeuterated in the methylene positions. General procedures for analyzing the thermolysis products were the same as for $Cp'_2Th[CH_2Si(CD_3)_3]_2$ (vide infra).

Table I. Summary of Thermolysis First-Order Rate Constants (s^{-1})

T, °C	k for **1**	k for **5**	k for **6**
50	1.05 (2) × 10^{-5}	1.38 (2) × 10^{-5}	1.50 (9) × 10^{-5}
60	3.23 (6) × 10^{-5}	3.41 (8) × 10^{-5}	3.20 (5) × 10^{-5}
70	7.30 (12) × 10^{-5}	8.41 (13) × 10^{-5}	8.21 (12) × 10^{-5}
80	2.00 (5) × 10^{-4}	1.95 (4) × 10^{-4}	1.84 (5) × 10^{-4}

T, °C	k for **3**	T, °C	k for **8**
70	3.89 (7) × 10^{-6}	70	6.1 (2) × 10^{-6}
85	2.08 (6) × 10^{-5}	80	1.47 (7) × 10^{-5}
100	8.3 (2) × 10^{-5}	90	3.66 (12) × 10^{-5}
115	3.21 (4) × 10^{-4}		

T, °C	k for **13**	k for process I	k for process II
85	3.13 (10) × 10^{-6}	2.09 (9) × 10^{-6}	1.04 (12) × 10^{-6}
95	1.05 (7) × 10^{-5}	6.9 (4) × 10^{-6}	3.6 (2) × 10^{-6}
105	1.38 (4) × 10^{-5}	1.5 (1) × 10^{-5}	8.8 (7) × 10^{-6}
115	6.40 (10) × 10^{-5}	3.8 (2) × 10^{-5}	2.6 (3) × 10^{-5}

$ClCH_2Si(CD_3)_3$. This is a modification of the literature procedure for $ClCH_2SiEt_3$.[23] A solution of 3.76 g (20.4 mmol, weighed by difference in an Ar-flushed syringe) of $ClCH_2SiCl_3$ in 50 mL of ether was added dropwise to a solution of 64 mmol of CD_3MgI in 50 mL of ether at 0 °C. A two-phase mixture resulted with a clear colorless fluid over a denser gray mixture. A clear, colorless solution over gray-white solids was obtained after ca. 12 h. Next, air was admitted to the flask, and sufficient dilute aqueous HCl was added to the mixture to dissolve all of the solids, the ether phase separated, and the aqueous phase extracted with 2 × 20 mL of ether. Iodine, which had formed during the workup, was removed at this point by washing the combined organic phases with a dilute aqueous solution of $Na_2S_2O_3$. After the solution was dried over $CaCl_2$ overnight, the product was isolated from the ether by fractional distillation in a microdistillation apparatus, bp 98–100 °C (literature for protio analogue, 98–99 °C). Residual iodine, indicated by a faint orange color, was removed by freeze–pump–thaw degassing over activated charcoal. The $ClCH_2Si(CD_3)_3$ was finally vacuum transferred to a storage tube containing P_2O_5, and after ca. 0.5 h of stirring, it was vacuum transferred to a tared storage tube; yield: 1.31 g (49%).

^1H NMR (C_6D_6): δ 2.75 (s, 2 H, $ClCH_2Si$), 0.13 (s, residual $SiCHD_2$ intensity indicates 0.13 H atoms per molecule: 99.7 atom % D); also 4% w/w diethyl ether.

$LiCH_2Si(CD_3)_3$. The compound $ClCH_2Si(CD_3)_3$ (1.31 g at 96% = 9.6 mmol) was metalated with lithium (1% Na) in heptane at 70 °C for 1 week. After filtration of the solution through Celite and concentration, crystallization at −78 °C gave 0.97 g (68%) of colorless needles of $LiCH_2Si(CD_3)_3$.

$Cp'_2Th[CH_2Si(CD_3)_3]_2$ (13). Starting with 0.50 g (4.85 mmol) of $LiCH_2Si(CD_3)_3$ and 1.14 g (1.99 mmol) of Cp'_2ThCl_2, **8** was synthesized in 80% yield according to the literature procedure[19] for $Cp'_2Th(CH_2SiMe_3)_2$. Before being used in kinetic experiments, this material was recrystallized twice, once with filtration through Celite. The temperature stability of **13** is markedly greater than that of **3**. It was found to be >99.6% CD_3 in the methyl groups by ^1H NMR and by hydrolysis, followed by GC–MS of the evolved neopentane.

Anal. Calcd for $C_{28}H_{34}D_{18}Si_2Th$: C, 48.54; H, 7.82. Found: C, 48.68; H, 7.73.

NMR Kinetics. All rate constants were determined by monitoring the Cp′ ^1H NMR resonances of reactions performed in NMR tubes, sealed in vacuo. In a typical experiment, a Wilmad 505 pp NMR tube sealed onto a 7.5-cm length of 5-mm Pyrex (to facilitate seal-off and subsequent reuse of the NMR tube) was charged with ca. 50 mg of solid reactant and ca. 0.4 mL of C_6D_{12} and sealed off in vacuo. After the sample was dissolved, an initial spectrum (t = 0 min) was recorded at room temperature, and the sample was then immersed in a thermostated Haake constant temperature bath filled with paraffin oil. At appropriate time intervals, the sample was removed from the oil bath, rinsed free of oil and cooled to −78 °C. The sample was next briefly warmed to record a room-temperature ^1H NMR spectrum (typically requiring less than 5 min) and then returned to the oil bath. Three Xerox copies were made of an expanded trace through the Cp′ region, and the extent of reaction was determined by cut and weigh integration. Each experiment was monitored for ca. 3 half-lives. Each rate constant was determined at least twice for each system and temperature studied. Plots of ln (A_0/A) vs. t were fit to eq 3 by the technique of least squares. Estimated standard

$$\ln (A_0/A) = kt + k_0 \qquad (3)$$

deviations for the regression parameters are based on the observed SSE and the variance covariance matrix. Observed rate constants are summarized in Table I.

Analysis of Products from Thermolysis of 13 by GC–MS. After each kinetic run for **13**, the NMR sample tube was brought into the glovebox and opened after scoring with a tungsten carbide glass knife. The open tube was quickly connected via a universal O-ring adaptor to a stopcock, brought out of the glovebox, and connected to the vacuum line. Three freeze–pump–thaw cycles were performed to degas the sample, and the volatiles from the reaction were collected in a separate tube. The tube containing the volatiles was then pressurized with Ar and opened to the atmosphere, and the collected liquid was transferred to a vial for subsequent GC–MS analysis. In a control experiment to check for abstraction of H from the solvent, the volatiles from thermolyses of **8** carried out both in protio cyclohexane at 85°C and in heptane were collected and analyzed by GC–MS. One of the samples from an 85 °C thermolysis in C_6D_{12}

---

(32) (a) Bruno, J. W.; Marks, T. J., unpublished results. (b) Bruno, J. W. Ph.D. Thesis, Northwestern University.

Table II. Results of GC-MS Analysis of Products of the Thermolysis of **13**

temp, °C	% Me_4Si-d_9[a]	% Me_4Si-d_{10}[a]	% Cp′-d_0[b]	% Cp′-d_1[b]
85	34 (4)	64 (4)		
	31 (3)	67 (3)		
95	34 (3)	64 (3)		
	34 (3)	65 (3)		
105	36 (4)	63 (4)	83 (2)	17 (2)
	37 (4)	61 (4)		
115	40 (4)	58 (4)		
	40 (5)	55 (5)		

[a] Volatile thermolysis product. [b] Hydrolysis (H_2O) product after completion of thermolysis.

Table III. Neutron-Diffraction Data Collection and Analysis Parameters

sample temp, K	50
space group	$P2_1/n$
unit cell parameters	
a, Å	11.206 (4)
b, Å	16.670 (6)
c, Å	15.742 (5)
β, deg	93.48 (2)
V, Å^3	2935 (3)
Z	4
approx crystal size, mm^3	4 × 4 × 2
linear absorption coeff, μ,[a] cm^{-1}	3.27
neutron wavelength, λ, Å	1.068 (3)
maximum 2θ angle, deg	90
type of data measured	$h,k,\pm l$
no. of prescanned data	10803
no. of scanned data[b]	3454
no. of unique reflections	2270
function minimized in l.s.	$\sum w(\lvert F_o\rvert - \lvert F_c\rvert)^2$
weights, w	$2F_o^2/(\sigma_{counting}^2 + (0.05F_o^2)^2)^{1/2}$
no. of variables	749
extinction parameters, g[c]	6.8 (3) × 10^{-5}
esd of an obs. of unit wt	2.05
final R factors	
$R(F)$	0.048
$wR(F)$	0.053

[a] Data were not corrected for absorption (see text). [b] Data with peak > 2(background) from prescan. [c] Extinction correction of the form $|F_c| = |F_o|(1 + gI_c)$.

was first hydrolyzed with a mixture of 0.5 mL of heptane and 0.2 mL of degassed H_2O and the volatiles then collected as above for analysis of the Cp′H by GC-MS.

Authentic Me_4Si-d_9 and Me_4Si-d_{10} samples were obtained by hydrolysis of the d_9 lithium reagent with H_2O and D_2O, respectively. The mass spectrum of authentic Cp′H-d_0 was obtained from a sample of Cp′H on hand. The fragmentation pattern of Cp′H-d_1 was simulated from the spectrum of Cp′H-d_0 by incrementing the observed m/e values by one and assuming that 1 of 5 Me groups lost contained a D atom.

In mass spectral analyses, observed mixtures were decomposed into contributions from the proposed isotopomers by a linear least-squares technique.[24-26] Each observed spectrum was normalized, and the spectra of mixtures were modeled by a linear combination of the spectra of the pure isotopic species and a constant dummy contribution. In all cases the dummy contribution accounted for less than 2% of the fit. For Me_4Si mixtures, intensities from m/e values of 77–85 inclusive were used; for Cp′H, intensities for m/e of 104–139 were used. In all cases, the intensity of each m/e peak was obtained by integrating the total intensity observed as the material eluted from the GC. The averages of the results from the determinations of each kinetic run are presented in Table II. Estimated standard deviations are based on the observed SSE and the variance covariance matrix. Representative fits are compared to observed spectra in Figure 1. In all cases the fits are significant at the 0.01 level.[25,26]

Neutron-Diffraction Study of $Cp'_2Th(CH_2CMe_3)_2$ (1).[20] Selected data collection and analysis parameters are provided in Table III. A yellow crystal of the compound was enclosed in a quartz glass tube with an argon atmosphere. The glass tube was mounted inside a helium-filled aluminum can which was threaded onto the cold stage of a Displex closed-cycle helium refrigerator. The temperature of the sample was maintained at 50 K throughout the data collection on the 2XE diffractometer (λ = 1.068 (3) Å) at the University of Missouri Research Reactor. Twenty-eight well-centered reflections with 30° ≤ 2θ ≤ 60° were used to determine the unit cell dimensions (see Table III). Reflections were scanned and integrated if, based on a rapid prescan measurement, the peak was greater than twice the background. Two check reflections were measured periodically throughout the data collection and showed no significant deviations. The data were corrected for Lorentz effects but not for absorption because of the difficulty in indexing the numerous crystal faces. Assuming a sphere of radius 0.2 cm, the relative absorption corrections would only vary by ±2% in the range 0° < θ < 45°.

Scheme II. Cyclometalation Reactions of Thorium Complexes

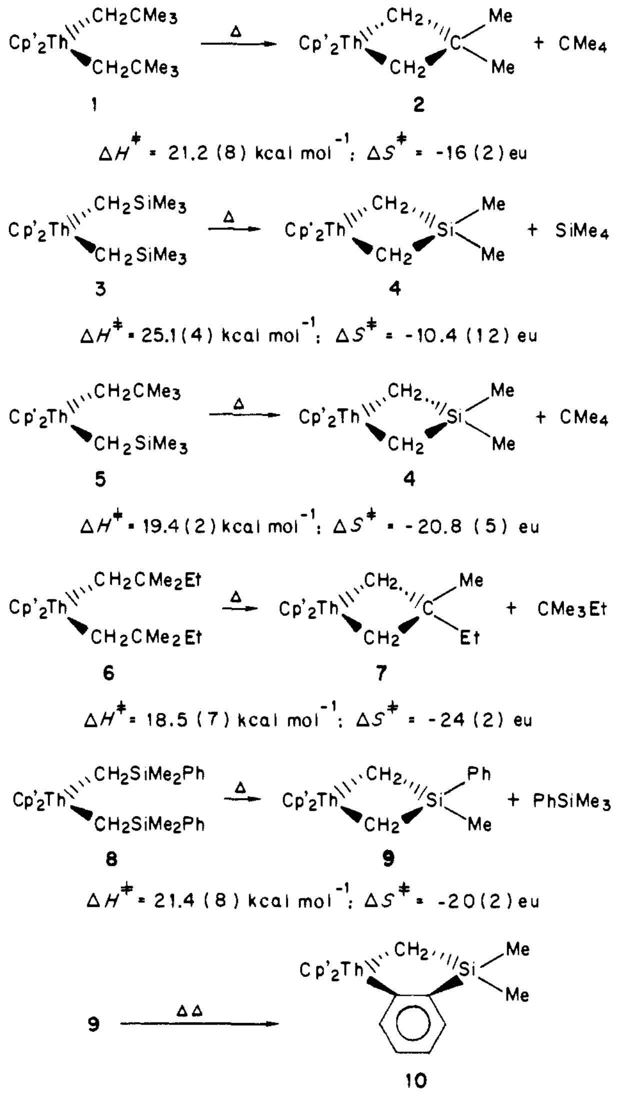

Approximately one-half of the hydrogen atoms were located in an initial difference Fourier map based on phases calculated from the positional parameters of the non-hydrogen atoms from the X-ray structure.[27] Subsequent alternations of least-squares refinements and Fourier maps yielded the remaining hydrogen atoms. In the final cycles of refinement, an extinction correction was included and all atoms were treated with anisotropic thermal parameters. The neutron scattering lengths for all atoms were taken from the tabulation by Bacon.[28] Most computations were carried out on a PDP 11/34 computer with Enraf-Nonius SDP-Plus 1.0 programs. Final atomic positional coordinates are presented in Table IV. The relatively large standard deviations for most of the parameters are probably mostly due to the poor observations-to-parameters ratio of 3.0. General temperature factor expressions are given in Table V.[20]

Results

Synthesis of Cp'_2ThR_2 Cyclometalation Precursors. The known bis(pentamethylcyclopentadienyl)thorium dialkyls **1** and **3** (see Scheme II for the complete compound numbering key) were prepared according to the literature procedures (eq 4 and 5).[19]

$$\mathrm{Cp'_2ThCl_2 + 2LiCH_2CMe_3 \xrightarrow{ether} \underset{\mathbf{1}}{Cp'_2Th(CH_2CMe_3)_2} + 2LiCl} \qquad (4)$$

$$\mathrm{Cp'_2ThCl_2 + 2LiCH_2SiMe_3 \xrightarrow{ether} \underset{\mathbf{3}}{Cp'_2Th(CH_2SiMe_3)_2} + 2LiCl} \qquad (5)$$

Analogous metathesis reactions were employed for the new thorium alkyls **5**, **6**, and **8** (eq 6–8). Thus, reaction of two equivalents of $LiCH_2CMe_2Et$ with Cp'_2ThCl_2 in a manner analogous to the literature method for **1** afforded **6** in 81% yield. The reaction

$$\mathrm{Cp'_2Th(CH_2SiMe_3)Cl + LiCH_2CMe_3 \xrightarrow{ether} \underset{\mathbf{5}}{Cp'_2Th(CH_2SiMe_3)(CH_2CMe_3)} + LiCl} \qquad (6)$$

$$\mathrm{Cp'_2ThCl_2 + 2LiCH_2CMe_2Et \xrightarrow{ether} \underset{\mathbf{6}}{Cp'_2Th(CH_2CMe_2Et)_2} + 2LiCl} \qquad (7)$$

$$\mathrm{Cp'_2ThCl_2 + 2LiCH_2SiMe_2Ph \xrightarrow{ether} \underset{\mathbf{8}}{Cp'_2Th(CH_2SiMe_2Ph)_2} + 2LiCl} \qquad (8)$$

of Cp'_2ThCl_2 with 2 equiv of $LiCH_2SiMe_2Ph$ in diethyl ether afforded **8** in 80% yield. The deuterated lithium reagents $LiCD_2CMe_3$, $LiCHDSiMe_3$, and $LiCH_2Si(CD_3)_3$ were prepared by the sequences outlined in Scheme III, using modifications of literature procedures for protio analogues or homologues.[21-24] Deuterated alkyls **11**, **12**, and **13** were then prepared as shown in eq 9–11. For use in kinetic isotope effect measurements, compound **13** was synthesized in 0.5-g quantities (80% isolated yield). It was found by ^{1}H NMR or, after hydrolysis, by GC–MS to have >99.6% substitution of D for H in the silylmethyl groups.

$$\mathrm{Cp'_2ThCl_2 + 2LiCHDSiMe_3 \xrightarrow{ether} \underset{\mathbf{11}}{Cp'_2Th(CHDSiMe_3)_2} + 2LiCl} \qquad (9)$$

$$\mathrm{Cp'_2ThCl_2 + 2LiCD_2CMe_3 \xrightarrow{ether} \underset{\mathbf{12}}{Cp'_2Th(CD_2CMe_3)_2} + 2LiCl} \qquad (10)$$

$$\mathrm{Cp'_2ThCl_2 + 2LiCH_2Si(CD_3)_3 \xrightarrow{ether} \underset{\mathbf{13}}{Cp'_2Th[CH_2Si(CD_3)_3]_2} + 2LiCl} \qquad (11)$$

All new complexes were characterized by elemental analysis and ^{1}H/^{13}C NMR spectroscopy. Relevant data can be found in the Experimental Section. Structural characterization of dialkyl complex **3**[14b] and the cyclometalation product **4**[14a] by single-crystal X-ray diffraction has already been reported. In the present contribution, we discuss, in detail, single-crystal neutron-diffraction results for compound **1** and allude to preliminary X-ray diffraction results for compounds **5** and **10** (full details will be reported elsewhere[29]).

Cyclometalation Products and Kinetics. The thermolyses of thorium dialkyl complexes **1**, **3**, **5**, **6**, and **8** in C_6H_{12} or C_6D_{12} was found to proceed as shown in Scheme II. Cyclometalation of **3**, **5**, and **8** (but not of **1** or **6**[30]) may also be carried out in aromatic hydrocarbons. The metallacycles **2**, **4**, **7**, and **9** were isolated in 65%, 75%, 68%, and 74% yields, respectively. Analyses, spectroscopic measurements, and an X-ray structure determination are all completely consistent with the assigned structures (vide infra). When the cyclometalation reactions are performed in C_6D_{12} and monitored by 270-MHz ^{1}H NMR, yields are essentially quantitative and no intermediates or signals attributable to species other than those indicated in Scheme II are observed. In this regard, the thermolysis of **6** was subjected to particular scrutiny since the analogous platinum-centered cyclometalation yields a metallacyclopentane[3a,b] and since three metallacyclic products are, a priori, possible (A–C). Monitoring the thermolysis of **6** by

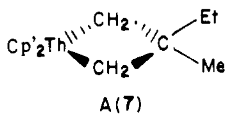
A(**7**)

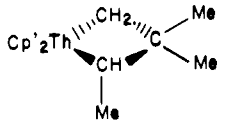
B

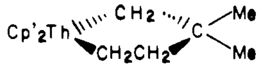
C

270-MHz ^{1}H NMR[20] reveals only signals due to **6**, **7**, and neohexane. Minor, broad resonances downfield of the Cp′ methyl region are also noted and are assignable to decomposition products arising from attack on ring methyl groups.[12,32] The ^{1}H NMR spectrum of **7** reveals magnetically inequivalent Cp′ rings, an ethyl group, a methyl group, and an AB quartet due to diastereotopic methylene protons. Of the three conceivable cyclometalation products, only structure A would exhibit the spectrum observed for **7**. On this basis, **7** is assigned structure A. Further confirmation that **7** is indeed a metallacycle is provided by a characteristic[12] ring-opening reaction with Me_4Si (eq 12). NMR monitoring[20] reveals that as the reaction proceeds, the Cp′ reso-

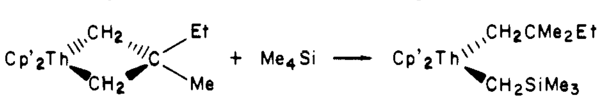
(12)

nances of the thoracycle decrease while a single new Cp′ resonance grows in. The final spectrum reveals a single product which contains magnetically equivalent Cp′ rings, a neohexyl functionality, and a (trimethylsilyl)methyl group. The resonances are easily assigned by comparing them to the corresponding spectral parameters for **5**, **1**, and **3** (see spectral data in the Experimental Section).

The thermal cyclometalation of **8** proceeds in a manner analogous to cyclometalation of **6**, yielding thoracyclobutane **9** (Scheme II). Figure 2 reproduces NMR spectra obtained during thermolysis of **8** in C_6D_6. As the reaction proceeds, **8** is converted into a compound with inequivalent Cp′ rings, a phenyl group, a methyl group, and diastereotopic methylene protons (Figure 2a–d). This is consistent with structural assignment **9**. The analogy to **6** ends here, however, as a new set of resonances grow in, at the expense of the resonances due to **9**, when the thermolysis is continued at higher temperatures (Figure 2d–f). It is apparent that the new thermolysis product derives solely from **9** since it continues to form, and **9** to decrease, after **8** has reacted completely. The ^{1}H and ^{13}C NMR spectra of this material suggest a formulation as structure **10**, which was confirmed by an X-ray structure determination (Figure 3A). The full details of the diffraction study will be discussed elsewhere.[29]

In contrast to the above results with complexes having β-branched alkyl groups, the thermolysis of $Cp'_2Th(CH_2CH_2CH_3)_2$ at 70 °C in C_6D_{12} (requiring 3 days) does not result in a stable thoracyclobutane. Monitoring by ^{1}H NMR reveals a final, complex pattern in the Cp′ region and broad resonances to low field of the Cp′ region (usually indicative of Cp′ methyl group attack[12,32]). There is no evidence during the reaction for any sort of product $\overline{ThCH_2CH_2CH_2}$ alkyl functionality. Examination of the volatiles produced by GC–MS reveals only propane-d_0, with insignificant (<3%) propane-d_1 or propene. Thus, there is no evidence for solvent hydrogen atom transfer to propyl groups or β-hydride elimination (the latter is expected to be thermodynamically unfavorable[15] but kinetically viable[12,32]). When the organometallic thermolysis product is treated with D_2O and the resulting volatiles trap-to-trap distilled, GC–MS reveals negligible propane, but a mixture of mono- and dideuteriopentamethylcyclopentadiene. This result indicates the presence, inter alia, of η^6-$(CH_3)_4C_5CH_2$ moieties presumably formed via Cp′ methyl hydrogen atom abstraction by an alkyl group (vide infra) or an unstable metallacycle.[12]

Kinetic information on the thermolyses of compounds **1**, **3**, **5**, **6**, **8**, **9**, and **13** was obtained on C_6D_{12} solutions sealed in vacuo

Table IV. Positional Parameters and Their Estimated Standard Deviations for $Cp'_2Th(CH_2CMe_3)_2$ (**1**)

atom	x	y	z	B_{eq} (Å^2)^a	atom	x	y	z	B_{eq} (Å^2)^a
Th	0.4993 (2)	0.2364 (1)	0.3060 (2)	0.56 (4)	H11B	0.292 (1)	0.2937 (6)	0.2539 (6)	2.5 (2)
C1A	0.5847 (4)	0.3082 (2)	0.1807 (3)	1.04 (8)	H21B	0.3764 (9)	0.3722 (6)	0.3019 (7)	2.7 (2)
C2A	0.5482 (4)	0.3868 (2)	0.1333 (3)	1.00 (8)	H13B	0.159 (1)	0.4283 (6)	0.2458 (8)	3.5 (2)
C3A	0.6296 (5)	0.4027 (3)	0.0608 (3)	1.64 (9)	H23B	0.087 (1)	0.3343 (7)	0.2430 (7)	3.0 (2)
C4A	0.4173 (4)	0.3812 (3)	0.0960 (3)	1.51 (8)	H33B	0.043 (1)	0.4118 (7)	0.3121 (8)	3.7 (2)
C5A	0.5560 (4)	0.4599 (3)	0.1932 (3)	1.29 (8)	H14B	0.300 (1)	0.4064 (6)	0.4681 (6)	3.0 (2)
C1B	0.3198 (4)	0.3193 (2)	0.3174 (3)	0.98 (8)	H24B	0.158 (1)	0.4489 (6)	0.4418 (7)	3.4 (2)
C2B	0.2068 (4)	0.3524 (2)	0.3556 (3)	1.05 (7)	H34B	0.279 (1)	0.4723 (6)	0.3793 (8)	3.6 (2)
C3B	0.1181 (4)	0.3834 (3)	0.2846 (3)	1.63 (9)	H15B	0.123 (1)	0.2359 (6)	0.3672 (7)	3.4 (2)
C4B	0.2386 (4)	0.4240 (3)	0.4141 (3)	1.52 (9)	H25B	0.067 (1)	0.3101 (7)	0.4317 (7)	3.1 (2)
C5B	0.1452 (4)	0.2876 (3)	0.4076 (3)	1.50 (9)	H35B	0.2070 (9)	0.2682 (6)	0.4599 (7)	2.8 (2)
CPA1	0.7158 (4)	0.2234 (2)	0.4053 (3)	1.24 (8)	H1MA1	0.807 (1)	0.1101 (6)	0.4011 (7)	3.1 (2)
CPA2	0.7083 (4)	0.3073 (2)	0.3850 (3)	1.16 (8)	H2MA1	0.8992 (9)	0.1928 (6)	0.3927 (8)	3.2 (2)
CPA3	0.6125 (4)	0.3400 (3)	0.4297 (3)	1.23 (8)	H3MA1	0.811 (1)	0.1601 (7)	0.3075 (7)	3.7 (2)
CPA4	0.5609 (4)	0.2764 (3)	0.4780 (3)	1.16 (8)	H1MA2	0.871 (1)	0.3739 (7)	0.3852 (7)	3.3 (2)
CPA5	0.6272 (4)	0.2056 (2)	0.4624 (3)	0.99 (8)	H2MA2	0.842 (1)	0.3168 (7)	0.2921 (8)	3.5 (2)
CMA1	0.8127 (4)	0.1695 (3)	0.3748 (3)	1.37 (8)	H3MA2	0.767 (1)	0.4069 (6)	0.3109 (8)	3.9 (2)
CMA2	0.8002 (4)	0.3535 (3)	0.3398 (3)	1.48 (9)	H1MA3	0.494 (1)	0.4392 (8)	0.437 (2)	8.0 (5)
CMA3	0.5831 (5)	0.4276 (3)	0.4360 (3)	1.60 (9)	H2MA3	0.619 (2)	0.4611 (7)	0.390 (1)	6.9 (4)
CMA4	0.4676 (4)	0.2838 (3)	0.5409 (3)	1.53 (9)	H3MA3	0.624 (2)	0.4532 (7)	0.489 (1)	6.5 (3)
CMA5	0.6133 (4)	0.1291 (3)	0.5127 (3)	1.63 (9)	H1MA4	0.500 (1)	0.265 (1)	0.6029 (8)	4.7 (3)
CPB1	0.3245 (4)	0.1270 (2)	0.2320 (3)	1.04 (8)	H2MA4	0.438 (1)	0.3461 (8)	0.5492 (8)	4.1 (3)
CPB2	0.3794 (4)	0.0876 (2)	0.3054 (3)	1.04 (8)	H3MA4	0.392 (1)	0.2463 (9)	0.5270 (8)	5.2 (3)
CPB3	0.4998 (4)	0.0695 (2)	0.2866 (3)	0.97 (8)	H1MA5	0.639 (1)	0.1409 (7)	0.5805 (7)	3.3 (2)
CPB4	0.5193 (4)	0.0979 (2)	0.2030 (3)	1.01 (8)	H2MA5	0.521 (1)	0.1055 (6)	0.5083 (7)	3.3 (2)
CPB5	0.4102 (4)	0.1331 (2)	0.1699 (3)	1.12 (8)	H3MA5	0.669 (1)	0.0809 (6)	0.4921 (7)	3.1 (2)
CMB1	0.1938 (4)	0.1447 (3)	0.2179 (3)	1.66 (9)	H1MB1	0.151 (1)	0.1004 (7)	0.1753 (8)	3.6 (2)
CMB2	0.3180 (4)	0.0666 (3)	0.3841 (3)	1.40 (8)	H2MB1	0.178 (1)	0.2032 (7)	0.1888 (9)	4.1 (3)
CMB3	0.5823 (4)	0.0132 (2)	0.3369 (3)	1.33 (8)	H3MB1	0.148 (1)	0.146 (1)	0.2741 (9)	5.0 (3)
CMB4	0.6287 (4)	0.0846 (3)	0.1553 (3)	1.52 (9)	H1MB2	0.379 (1)	0.041 (1)	0.4339 (8)	5.0 (3)
CMB5	0.3839 (5)	0.1584 (3)	0.0783 (3)	1.58 (9)	H2MB2	0.275 (2)	0.1160 (8)	0.4102 (8)	4.2 (3)
H11A	0.6791 (8)	0.3123 (6)	0.1979 (7)	2.4 (2)	H3MB2	0.254 (1)	0.0216 (9)	0.3717 (8)	6.4 (3)
H21A	0.578 (1)	0.2611 (6)	0.1322 (6)	2.7 (2)	H1MB3	0.673 (1)	0.0328 (6)	0.3428 (8)	3.4 (2)
H13A	0.608 (1)	0.4589 (6)	0.0286 (7)	3.4 (2)	H2MB3	0.559 (1)	0.0038 (8)	0.4012 (8)	4.2 (3)
H23A	0.7232 (9)	0.4059 (7)	0.0842 (7)	2.8 (2)	H3MB3	0.580 (1)	−0.0462 (6)	0.3078 (8)	3.8 (3)
H33A	0.624 (1)	0.3540 (7)	0.0142 (7)	3.8 (2)	H1MB4	0.619 (1)	0.0340 (7)	0.1127 (8)	4.1 (2)
H14A	0.394 (1)	0.4350 (6)	0.0588 (7)	3.2 (2)	H2MB4	0.654 (1)	0.1363 (6)	0.1186 (8)	4.3 (2)
H24A	0.409 (1)	0.3293 (6)	0.0522 (7)	3.2 (2)	H3MB4	0.707 (1)	0.0708 (9)	0.1968 (8)	4.6 (3)
H34A	0.352 (1)	0.3713 (7)	0.1444 (7)	3.6 (2)	H1MB5	0.356 (1)	0.1077 (6)	0.0398 (7)	4.2 (3)
H15A	0.528 (1)	0.5150 (5)	0.1589 (7)	2.9 (2)	H2MB5	0.462 (1)	0.1856 (8)	0.0522 (7)	3.7 (2)
H25A	0.646 (1)	0.4692 (7)	0.2196 (8)	3.6 (2)	H3MB5	0.314 (1)	0.2027 (7)	0.0735 (7)	3.8 (2)
H35A	0.496 (1)	0.4521 (6)	0.2462 (7)	3.0 (2)					

[a] Anisotropically refined atoms are given in the form of the isotropic equivalent thermal parameter defined as $B_{eq} = {}^4/_3\sum_i\sum_j\beta_{ij}\mathbf{a}_i\cdot\mathbf{a}_j$.

Scheme III. Synthetic Procedures Used To Obtain Labeled Alkyl Ligands

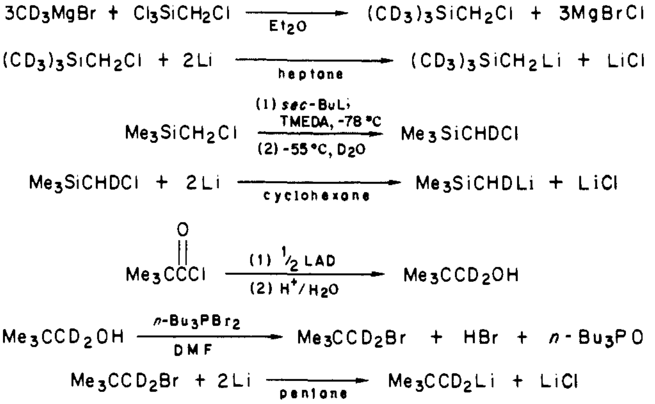

$$3CD_3Br + \text{excess Mg} \xrightarrow[Et_2O]{} 3CD_3MgBr$$

$$3CD_3MgBr + Cl_3SiCH_2Cl \xrightarrow[Et_2O]{} (CD_3)_3SiCH_2Cl + 3MgBrCl$$

$$(CD_3)_3SiCH_2Cl + 2Li \xrightarrow[\text{heptone}]{} (CD_3)_3SiCH_2Li + LiCl$$

$$Me_3SiCH_2Cl \xrightarrow[(2)\ -55\ ^\circ C,\ D_2O]{(1)\ sec\text{-BuLi}\ \text{TMEDA},\ -78\ ^\circ C} Me_3SiCHDCl$$

$$Me_3SiCHDCl + 2Li \xrightarrow[\text{cyclohexone}]{} Me_3SiCHDLi + LiCl$$

$$Me_3C\overset{\overset{O}{\|}}{C}Cl \xrightarrow[(2)\ H^+/H_2O]{(1)\ {}^1/_2\ LAD} Me_3CCD_2OH$$

$$Me_3CCD_2OH \xrightarrow[DMF]{n\text{-}Bu_3PBr_2} Me_3CCD_2Br + HBr + n\text{-}Bu_3PO$$

$$Me_3CCD_2Br + 2Li \xrightarrow[\text{pentone}]{} Me_3CCD_2Li + LiCl$$

in 5-mm NMR tubes. The progress of the reactions was monitored by the relative intensities of the various Cp′ resonances in the ^{1}H NMR. Good first-order behavior was observed over at least 3 half-lives, and rate constants, derived from least-squares analysis of the data, are set out in Table I. Rates were typically measured for each cyclometalation reaction at four temperatures over a range of 30 °C. Eyring plots of these data are shown in Figure 4, and activation parameters obtained from a least-squares analysis of these plots are given in Scheme II. It can be seen that the $\Delta H^‡$ and $\Delta S^‡$ values are rather similar for all of the cyclometalation reactions. The rather large, negative entropies of activation are particularly conspicuous.

Isotopic Labeling Experiments. A number of deuterium-labeled thorium dialkyls were synthesized and GC–MS analyses of the thermolysis products carried out to trace the fate of various hydrogen atoms in the Cp'_2ThR_2 framework upon thermolysis. In addition to these experiments, volatiles from the cyclometalation reactions of all-protio **1** and **3** in C_6D_{12} were analyzed to test for solvent C–D involvement. Figure 1 reproduces some of the mass spectra and, along with Scheme IV, summarizes the results of the labeling experiments. Thermolysis of **1** or **3** in C_6D_{12} yields neopentane and Me_4Si, respectively, which incorporate no excess deuterium (≤1%). Furthermore, thermolysis of **11** and **12** yields products which give no evidence of α-hydrogen abstraction processes. Thus, GC–MS analysis of the volatiles from these reactions gives mass spectra of neopentane and Me_4Si which are indistinguishable from those of the labeled neopentane or Me_4Si obtained from hydrolysis (H_2O) of the deuterated thorium alkyls **11** and **12**. Thermolysis of **13** was studied in somewhat greater detail as it was apparent, even in synthesis of **13**, that substitution of D or H on the Si methyl groups slowed the rate of cyclometalation significantly.

In the rate data for the thermolysis of **3** vs. **13** (Table I), a large kinetic isotope effect is observed: k_H/k_D = 6.6 (2) at 85 °C and 5.0 (1) at 115 °C. This kinetic deuterium isotope effect suggests that a mechanism such as A (Scheme V) involving rate-limiting γ-hydrogen abstraction is operative. If so, the volatiles should contain exclusively $CH_2DSi(CD_3)_3$ (Me_4Si-d_{10}). On the other

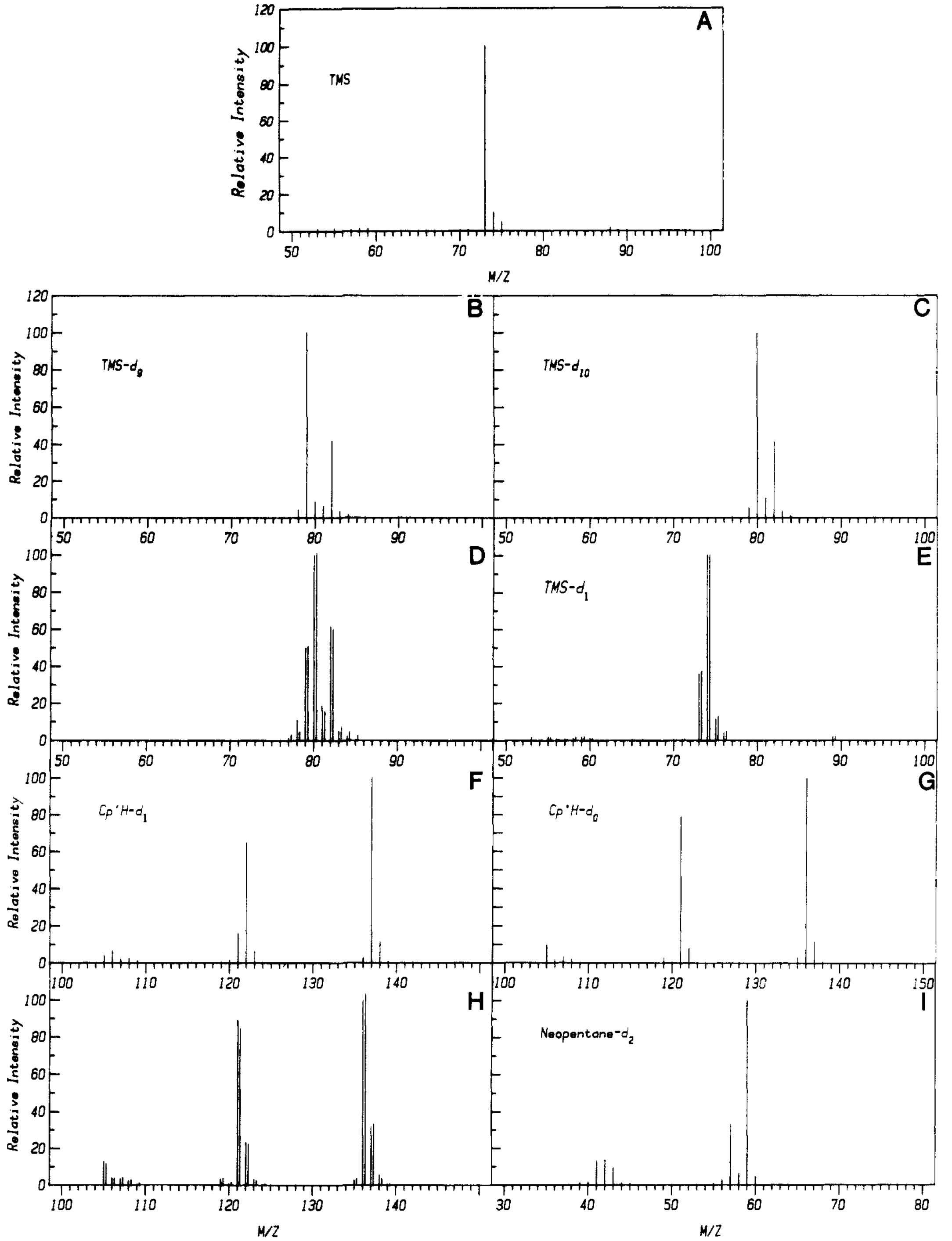

Figure 1. Selected mass spectra obtained in the GC–MS analyses. (A) 90 eV EI spectrum of Me_4Si formed in thermolysis of **3** in C_6D_6. The strong peak at *m/e* 73 is due to Me_3Si^+. At *m/e* 74 is the peak due to the natural isotopic abundance of ^{13}C, ^2H, and ^{29}Si: calculated 9.6% relative intensity, observed 9.8%. (B) Mass spectrum of Me_4Si-d_9 obtained by hydrolysis of $LiCH_2Si(CD_3)_3$. The intense peaks are due to $(CD_3)_3Si^+$ *m/e* 82 and $MeSi(CD_3)_2^+$ *m/e* 79. (C) Mass spectrum of Me_4Si-D_{10} obtained by hydrolysis with D_2O of $LiCH_2Si(CD_3)_3$. The intense peaks are due to $(CD_3)_3Si^+$ and $(CH_2D)(CD_3)_2Si^+$ *m/e* 80. (D) Mass spectrum of Me_4Si obtained in a thermolysis of **3** (leftmost lines) compared to a calculated spectrum from a least-squares fit (rightmost lines). (E) 90 eV mass spectrum of Me_3SiCH_2D obtained in thermolysis of **11** (rightmost lines) and obtained from hydrolysis of **11** (leftmost lines). Note that the peaks at *m/e* 73 and 74 occur in the expected 1:3 ratio (observed 35.9:100) and that the *m/e* 74 peak occurs with 11.6% relative intensity (calculated based on Me_4Si-d_0 fragmentation pattern: 11.5%). (F) Mass spectrum calculated for Cp'H-d_1 as described in the text. (G) Spectrum observed for Cp'H-d_0. (H) Observed (leftmost line) and calculated (rightmost line) mass spectra for Cp'H obtained upon hydrolysis of the products from cyclometalation of **12** at 85 °C. (I) 25 eV mass spectrum of neopentane obtained in the thermolysis of **12**. The fragments $Me_2(CD_2H)C^+$ *m/e* 59 and Me_3C^+ *m/e* 57 occur in the expected 3:1 ratio (observed 3.04:1.00). Material obtained from hydrolysis of **12** gives an identical ratio for these two fragments.

hand, volatiles from a reaction involving a ring hydrogen atom abstraction mechanism such as B should contain only $CH_3Si(CD_3)_3$ (Me_4Si-d_9). Analysis of the Me_4Si from the thermolysis of **13** by GC–MS shows (Scheme IV) that in fact a mixture of Me_4Si-d_9 and Me_4Si-d_{10} is formed. Similar mixtures of these components were observed at all temperatures, and identical compositions were observed in both deuterated and nondeuterated solvents. With use of spectra of authentic Me_4Si-d_9 and Me_4Si-d_{10} samples as a basis set, the observed mass spectra of Me_4Si from the thermolyses were successfully modeled by least-squares techniques (see Figure 1). The composition of these mixtures is summarized in Table II. The observation that hydrolysis of the products from thermolysis of **13** at 105 °C gives a mixture of 83 (2)% Cp'-d_0 and 17 (2)% Cp'-d_1[33] is consistent with a model of

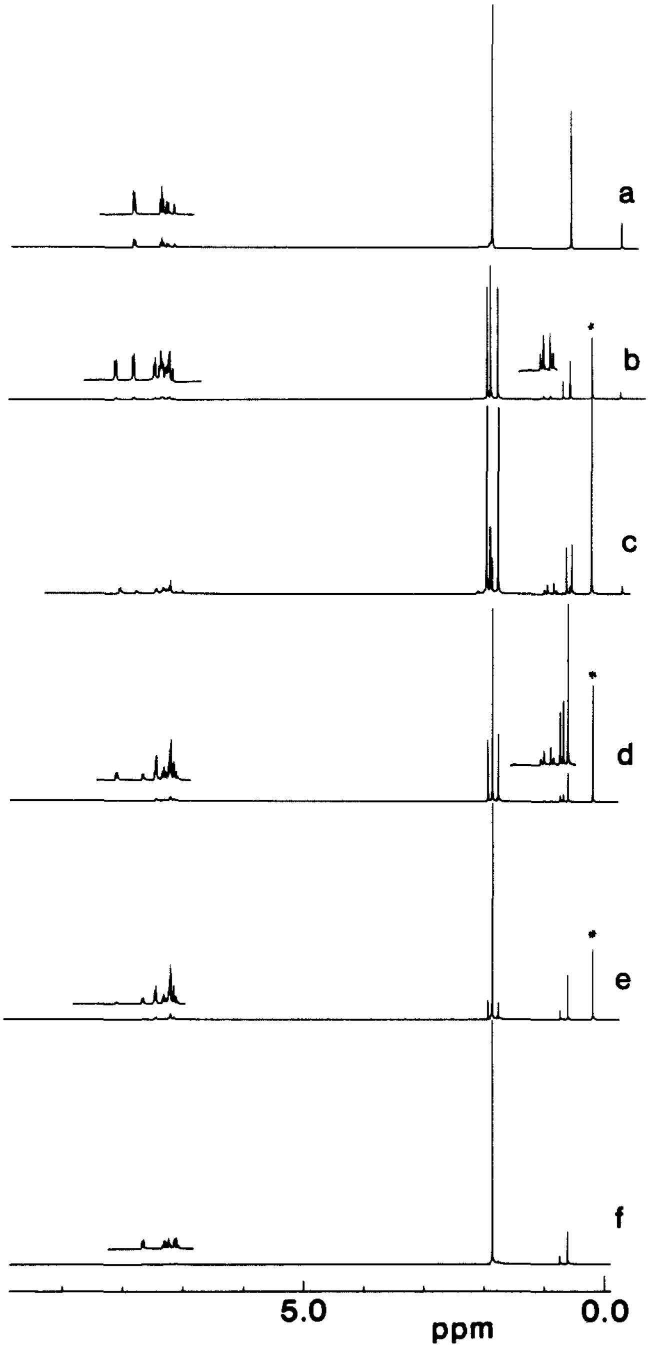

Figure 2. ^{1}H NMR spectra (270 MHz) obtained during thermolysis of **8** in C_6D_6 which shows stepwise formation of **9** and **10**: (a) pure **8** in C_6D_6; (b) formation of **9** in progress, * = methyl resonance of evolved phenyltrimethylsilane; (c) nearly complete formation of **9** showing inequivalent Cp' ligands and diastereotropic methylene protons; (d) formation of **10** in progress; (e) thermolysis complete; (f) pure **10** for comparison.

competing pathways I and II in Scheme IV (mechanism A and B in Scheme V) in the thermolysis of **3**/**13**. Thus, thermolysis at 105 °C yields Me_4Si which contains 36–37% Me_4Si-d_9. Since a D atom can be transferred to only one of the two Cp' rings on each molecule forming Me_4Si-d_9, there should be 36/2 ~ 18% Cp'-d_1 formed. This is within the experimental error of the observed amount.

If processes I and II (Scheme IV) are both first order in **13** and both lead to **4**, which is reasonable in view of the observed first-order kinetics, it is possible to use the present data to calculate rate constants and activation parameters for the individual component processes.[34] These results are summarized in Table I and Scheme IV. It is noteworthy that the activation parameters for Cp' hydrogen abstraction differ significantly from those for all processes involving alkyl-group γ-hydrogen abstraction.[35]

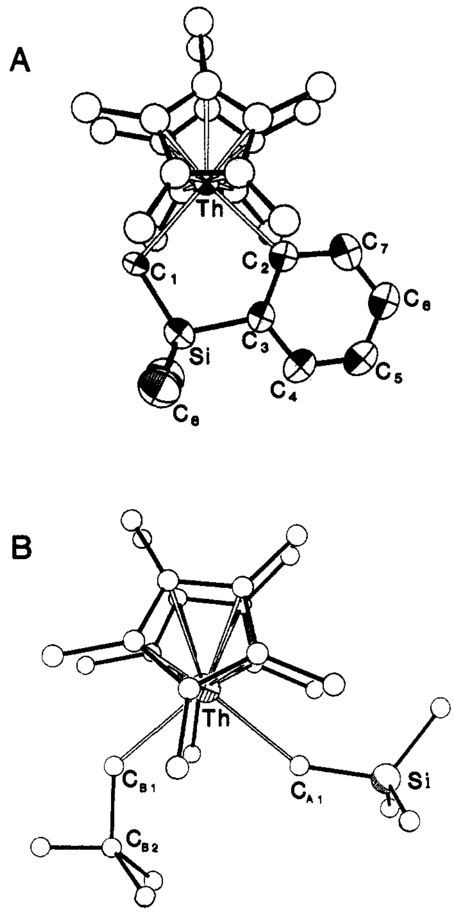

Figure 3. (A) Perspective view of the molecular structure of $Cp'_2ThCH_2SiMe_2$-*o*-C_6H_4). Some important bond lengths (Å) and angles (deg): Th–C_1 = 2.493 (11), Th–C_2 = 2.449 (12), Si–C_2 = 1.850 (11), Si–C_3 = 1.898 (13), C_1–Th–C_2 = 86.3 (4), Th–C_1–Si = 106.9 (5), Th–C_2–C_3 = 113.6 (8). (B) Perspective view of the molecular structure of $Cp'_2Th(CH_2CMe_3)(CH_2SiMe_3)$ (**5**). Some important bond lengths (Å) and angles (deg) include the following: Th–C_{a1} = 2.47 (3), Th–C_{b1} = 2.44 (3), ThC_{a1}–Si = 150 (3), Th–C_{b1}–C_{b2} = 132 (3), C_{a1}–Th–C_{b1} = 101 (3).[29]

Although the kinetic and isotopic labeling studies provide much information on the dynamics of the cyclometalation process, relevant structurally related questions arise concerning thermodynamics and regiospecificity. It was noted in our thermochemical work[15] that the first Th–CH_2CMe_3 bond in **1** (and to some degree, the first Th–CH_2SiMe_3 bond in **2**) possessed relatively low bond disruption enthalpies. This feature works to balance the unfavorable effects of thoracyclobutane ring strain and to render cyclometalation thermodynamically more favorable. Furthermore, the X-ray diffraction-derived molecular structure **3**[14b] revealed a curious distortion in one Th–C(α)–Si bond angle and a rather close C(α)–C(γ) contact (D). To the extent that such structural features might be related to unusual bonding situations and to

---

[33] For this fit, R^2 = 0.997, the best fit obtained in the course of analyzing the MS data, which we take as strong evidence that there is little or no Cp'H-d_n, $n \geq 2$, in the mixture.

[34] In this case, $k_{obsd} = k_I + k_{II}$ where k_{obsd} is the overall rate constant observed for cyclometalation of **13**, k_I is the rate constant for process I, and k_{II} is the rate constant for process II. Since both processes are unimolecular and arise from the same species, % process I/% process II = k_I/k_{II}. This gives two equations in two unknowns which may be solved by simple algebra.

[35] We assume that ring hydrogen atom abstraction rather than alkyl hydrogen atom abstraction is rate-limiting. If the former step were significantly reversible, polydeuterated Cp' ligands would be detected.

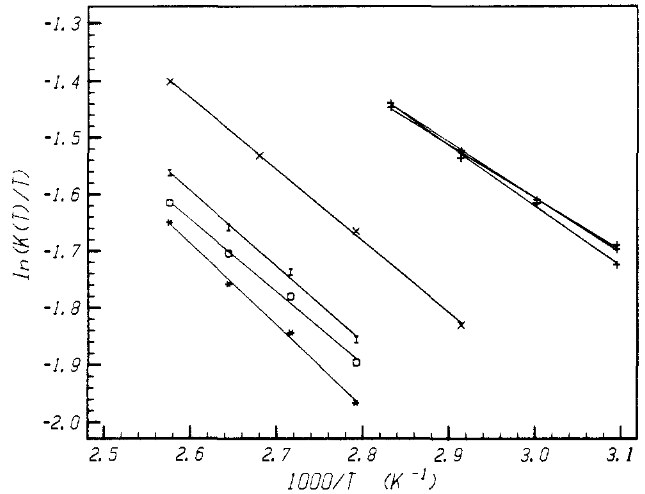

Figure 4. Eyring equation plots for cyclometalation reactions: + = **1** → **2**, **5** → **4**, and **6** → **7**; I = **3** → **4**; X = **13**, O = process I, * = process II.

Scheme IV. Restuls of Deuterium-Labeling Experiments

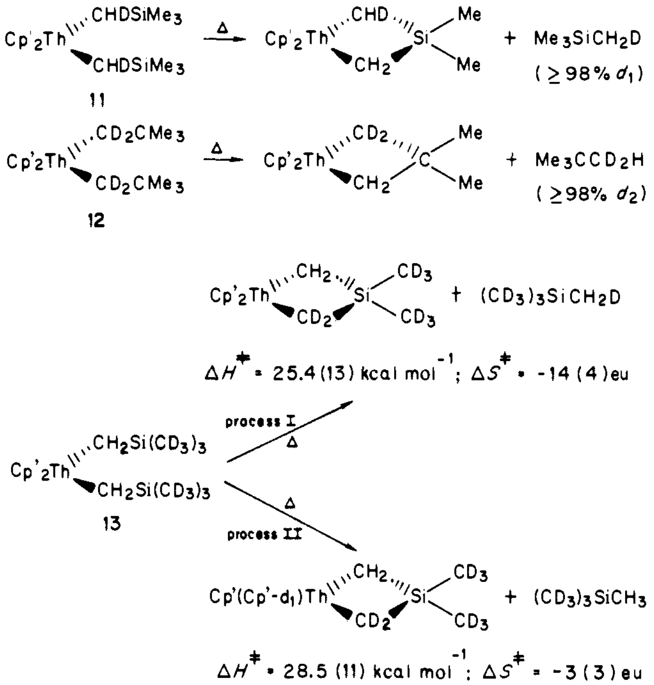

the regiospecificity of hydrogen atom transfer, the hydrogen atom positions in such molecules were of obvious interest.

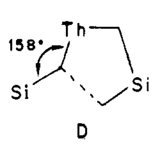

D

Neutron-Diffraction Study of Cp$'_2$Th(CH$_2$CMe$_3$)$_2$ (1). Bond distances and angles for the neutron-diffraction structure at 50 K are given in Table VI. A perspective view of the molecule is shown in Figure 5 and a stereoview is shown in Figure 6. The molecule has a typical Cp$'_2$MX$_2$ "bent sandwich" geometry with a ring centroid–Th–ring centroid angle of 130.0°. The average Th–C(ring) distance of 2.836 (4, 4, 4, 10)[36] Å, average C(ring)–C(ring) distance of 1.428 (5, 5, 6, 10) Å, and average C(ring)–CH$_3$(ring) distance of 1.502 (5, 5, 6, 10) Å are all unexceptional for a Cp$'_2$ThX$_2$ complex.[14a,g,37] The dihedral angle between the ring centroid–Th–ring centroid plane and the C$_{1A}$–Th–C$_{1B}$ "equatorial girdle" plane of 90.1° is also typical of such molecules.

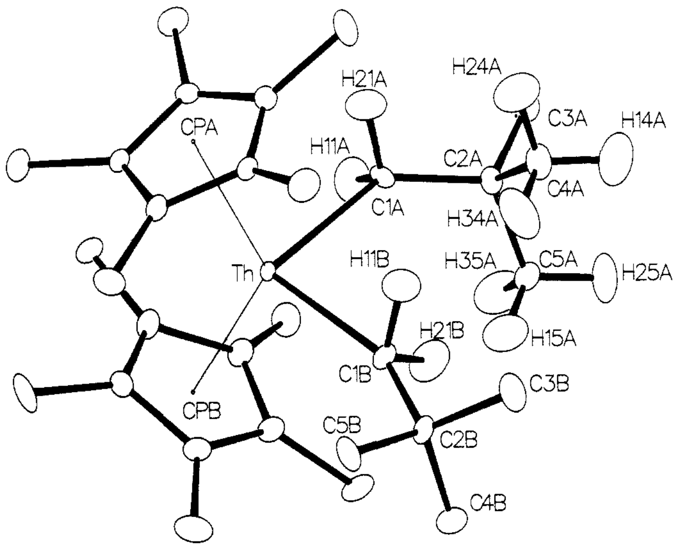

Figure 5. Perspective drawing of the 50 K neutron diffraction structure of Cp$'_2$Th(CH$_2$CMe$_3$)$_2$ (**1**). For clarity, methyl hydrogen atoms on the neopentyl and cyclopentadienyl ligands are not included.

Scheme V. Possible Mechanisms for Cyclometalation Processes in Cp$'_2$ThR$_2$ Complexes

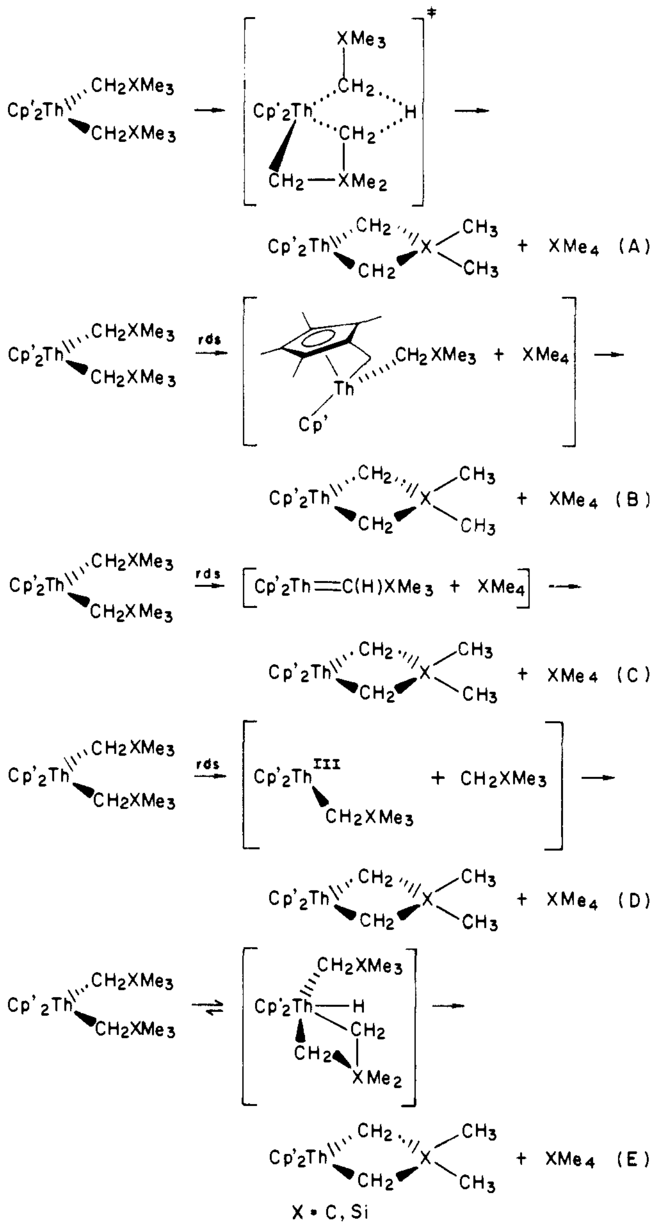

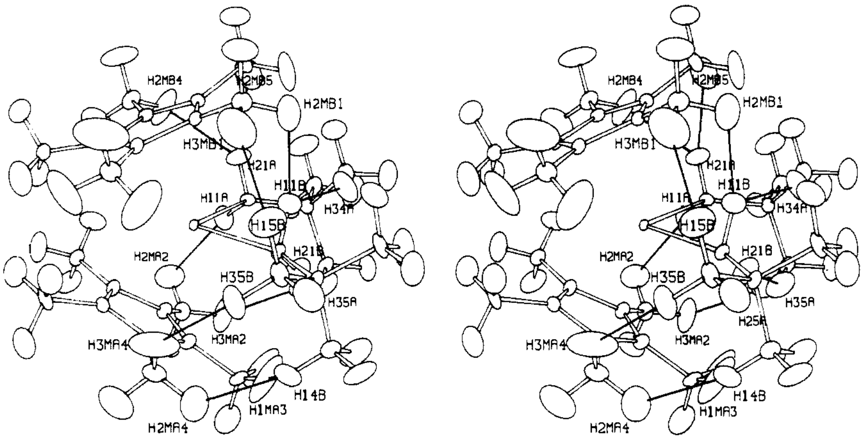

Figure 6. Stereoview of the 50 K neutron diffraction structure of $Cp'_2Th(CH_2CMe_3)_2$ (**1**), including all hydrogen atoms. Intramolecular neopentyl–neopentyl and neopentyl–cyclopentadienyl H–H contacts of less than 2.4 Å are shown as thin solid lines.

With regard to the $Th(CH_2CMe_3)_2$ ligation, the C_{1A}–Th–C_{1B} angle of 98.1 (1)° is typical of Cp'_2ThX_2 compounds.[14a,b,36] However, the exact disposition of the neopentyl ligands is reminiscent of **3** (D)[14b] and evidences severe distortions. As found in **3**, the vectors bisecting the Th–C_{1A}–C_{2A} and the Th–C_{1B}–C_{2B} angles point in the same general direction in the "equatorial girdle". The Th–C_{1A}–C_{1B} angle of 132.1 (3)°, while greater than tetrahedral, is not unusual for an f-element hydrocarbyl.[14a,37] As in **3**, the alkyl group with the more normal Th–C(α)–C(β) angle is oriented so that the bisector of this angle points toward the ring centroid–Th–ring centroid plane (the "knee" points away from this plane). The dihedral angle between the C_{1A}–Th–C_{1B} and C_{2A}–C_{1A}–Th planes is 8.3°, i.e., as viewed in Figure 5, the C_{2A}–C_{1A}–Th plane is twisted 8.3° counterclockwise about the $C_{1A}\rightarrow$Th vector from the C_{1A}–Th–C_{1B} plane. Atom C_{2A} lies 0.17 Å below the equatorial girdle as viewed in Figure 5. The Th–C_{1A}–H_{11A} and Th–C_{1A}–H_{21A} angles of 104.2 (6)° and 101.1 (5)°, respectively, are only slightly contracted from tetrahedral, while the C_{1A}–H_{11A} and C_{1A}–H_{21A} distances 1.079 (11) and 1.095 (8) Å, respectively, are reasonable for aliphatic C–H distances (1.096 (2) Å in CH_4,[38a] 1.107 (1) Å in C_2H_6[38b]). The Th–C_{1A} distance of 2.543 (4) Å can be compared to Th–C σ bond distances of 2.51 (1) Å for the "normal" CH_2SiMe_3 group of **3**, 2.463 (13) Å in **4**,[14a] 2.55 (2) Å (average) in $Th(benzyl)_4(dmpe)_2$,[39] and 2.571 (9) Å for the terminal Th–CH_3 group in $[Li(TMEDA)]_3Th(CH_3)_7\cdot TMEDA$.[40]

Table VI. Interatomic Distances (Å) and Angles (deg) in the Neutron Structure of $Th(C_5Me_5)_2(CH_2CMe_3)_2$ (**1**)

	(a) Distances		
Th–C_{1A}	2.543 (4)	Th–C_{1B}	2.456 (4)
C_{1A}–C_{2A}	1.551 (5)	C_{1B}–C_{2B}	1.536 (5)
C_{1A}–H_{11A}	1.079 (11)	C_{1B}–H_{11B}	1.114 (9)
C_{1A}–H_{21A}	1.095 (8)	C_{1B}–H_{21B}	1.122 (8)
Th–C_{PA1}	2.813 (4)	Th–C_{PB1}	2.872 (4)
Th–C_{PA2}	2.842 (4)	Th–C_{PB2}	2.822 (4)
Th–C_{PA3}	2.842 (4)	Th–C_{PB3}	2.799 (4)
Th–C_{PA4}	2.832 (4)	Th–C_{PB4}	2.839 (4)
Th–C_{PA5}	2.819 (4)	Th–C_{PB5}	2.881 (4)
C_{2A}–C_{3A}	1.527 (6)	C_{2B}–C_{3B}	1.540 (5)
C_{2A}–C_{4A}	1.549 (5)	C_{2B}–C_{4B}	1.536 (5)
C_{2A}–C_{5A}	1.540 (5)	C_{2B}–C_{5B}	1.543 (5)
C_{PA1}–C_{PA2}	1.436 (5)	C_{PB1}–C_{PB2}	1.436 (5)
C_{PA2}–C_{PA3}	1.427 (6)	C_{PB2}–C_{PB3}	1.431 (5)
C_{PA3}–C_{PA4}	1.445 (5)	C_{PB4}–C_{PB4}	1.428 (5)
C_{PA4}–C_{PA5}	1.424 (5)	C_{PB4}–C_{PB5}	1.426 (5)
C_{PA5}–C_{PA1}	1.411 (6)	C_{PB5}–C_{PB1}	1.415 (6)
av C–H[a]	1.079 (22)	av C_P–C_M	1.502 (9)
Th–H_{11A}	2.996 (9)	Th–H_{11B}	2.597 (9)
Th–H_{21A}	2.956 (9)	Th–H_{21B}	2.648 (9)
	(b) Angles		
C_{1A}–Th–C_{1B}	98.1 (1)	C_{1B}–Th–C_{PA}[b]	108.3 (1)
C_{1A}–Th–C_{PA}[b]	104.3 (1)	C_{1B}–Th–C_{PB}[b]	105.8 (1)
C_{1A}–Th–C_{PB}[b]	102.6 (1)	C_{PA}–Th–C_{PB}[b]	133.0 (1)
Th–C_{1A}–C_{2A}	132.1 (3)	Th–C_{1B}–C_{2B}	158.2 (3)
Th–C_{1A}–H_{11A}	104.2 (6)	Th–C_{1B}–H_{11B}	84.4 (5)
Th–C_{1A}–H_{21A}	101.1 (5)	Th–C_{1B}–H_{21B}	87.1 (5)
C_{2A}–C_{1A}–H_{11A}	107.1 (5)	C_{2B}–C_{1B}–H_{11B}	107.3 (5)
C_{2A}–C_{1A}–H_{21A}	105.4 (5)	C_{2B}–C_{1B}–H_{21B}	107.1 (5)
H_{11A}–C_{1A}–H_{21A}	103.9 (8)	H_{11B}–C_{1B}–H_{21B}	103.7 (7)
C_{1A}–C_{2A}–C_{3A}	110.7 (3)	C_{1B}–C_{2B}–C_{3B}	110.3 (3)
C_{1A}–C_{2A}–C_{4A}	110.3 (3)	C_{1B}–C_{2B}–C_{4B}	110.3 (3)
C_{1A}–C_{2A}–C_{5A}	111.7 (3)	C_{1B}–C_{2B}–C_{5B}	111.3 (3)
av C_P–C_P–C_P	108.0 (9)	av C–C–H[a]	111.7 (15)
av C_M–C_P–C_P	125.7 (15)	av H–C–H[a]	107.1 (20)

[a] The neopentyl α-C and α-H atoms are not included. [b] C_{PA} and C_{PB} denote the centroids of the A and B cyclopentadienyl ligands, respectively.

In contrast to the "normal" neopentyl ligand, the Th–C_{1B}–C_{2B} "knee" points inward toward the ring centroid–Th–ring centroid plane (as in **3**) with a remarkably obtuse angle of 158.2 (3)° (the corresponding angle in **3** is 148.0 (7)°). The Th–C_{1B}–C_{2B} plane is twisted 10.3° counterclockwise about the $C_{1B}\rightarrow$Th vector from the C_{1A}–Th–C_{1B} plane. Atom C_{2B} lies 0.10 Å below the equatorial girdle as viewed in Figure 5. The ∠Th–C_{1B}–C_{2B} distortion is accompanied by a rather short Th–C_{1B} distance of 2.456 (4) Å (the corresponding short distance in **3** is 2.46 (1) Å). In addition, C_{1B}–C_{2B} at 1.536 (5) Å may be slightly shorter than C_{1A}–C_{2A} at 1.551 (5) Å (this is at the boundary of statistical significance). The neutron-diffraction results reveal that vectors C_{1B}–H_{11B} and C_{1B}–H_{21B} point toward the ring centroid–Th–ring centroid plane and are "bent" toward the thorium center with ∠Th–C_{1B}–H_{11B} = 84.4 (5)° and ∠Th–C_{1B}–H_{21B} = 87.1 (5)°. The H_{11B}–C_{1B}–H_{21B} angle is a somewhat small 103.7 (7)°. Although it is probably at the boundary of statistical significance it is noteworthy that the distances C_{1B}–H_{11B} = 1.114 (9) Å and C_{1B}–H_{21B} = 1.122 (8) Å appear to be longer than typical aliphatic C–H bonds and the

---

(36) The first number in parentheses following an averaged value of a bond length or angle is the root-mean-square estimated standard deviation of an individual datum. The second and third numbers, when given, are the average and maximum deviations from the averaged value, respectively. The fourth number represents the number of individual measurements which are included in the average value.

(37) (a) Marks, T. J.; Day, V. W. In "Fundamental and Technological Aspects of Organo-f-Element Chemistry"; Marks, T. J., Fragalà, I. L., Eds.; Reidel: Dordrecht, 1985; pp 115–157. (b) Marks, T. J.; Ernst, R. D. In "Comprehensive Organometallic Chemistry"; Wilkinson, G., Stone, F. G. A., Abel, E. W., Eds.; Pergamon Press: Oxford, 1982; Chapter 21. (c) Marks, T. J. *Science* **1982**, *217*, 989–997. (d) Fagan, P. J.; Manriquez, J. M.; Marks, T. J.; Vollmer, S. H.; Day, C. S.; Day, V. W. *J. Am. Chem. Soc.* **1981**, *103*, 2206–2220. (e) Marks, T. J.; Manriquez, J. M.; Fagan, P. J.; Day, V. W.; Day, C. S.; Vollmer, S. H. *ACS Symp. Ser.* **1980**, *131*, 1–29.

(38) (a) Kuchitsu, K. *J. Chem. Phys.* **1968**, *49*, 4456–4462. (b) Bartell, L. S.; Kuchitsu, K.; De Neui, R. J. *J. Chem. Phys.* **1965**, *35*, 1211–1218.

(39) Edwards, P. G.; Andersen, R. A.; Zalkin, A. *Organometallics* **1984**, *3*, 293–299.

(40) Lauke, H.; Swepston, P. N.; Marks, T. J. *J. Am. Chem. Soc.* **1984**, *106*, 6841–6843.

corresponding bonds in the other neopentyl ligand (C_{1A}–H_{11A} = 1.079 (11) Å, C_{1A}–H_{21A} = 1.095 (8) Å). The Th–H_{11B} and Th–H_{21B} distances of 2.597 (9) and 2.648 (9) Å, respectively, are 0.31–0.35 Å longer than the Th–H(bridge) distance of 2.29 (3) Å in the neutron structure of $[Cp'_2Th(\mu\text{-}H)H]_2$.[41] Taken together, these features of an opened M–C(α)–C(β) angle, a shortened M–C(α) distance, an acute M–C(α)–H angle, and expanded C(α)–H distances are strikingly reminiscent of high-valent early transition-metal alkylidene structures (E) where ∠M–C–R ~ 140–170° and ∠M–C–H ~ 80°.[42] Although in the present case

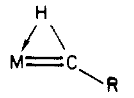
E

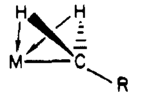
F

the shortened M–C distance would seem most likely attributable to rehybridization ($sp^3 \rightarrow sp$) accompanying the expanded Th–C(α)–C(β) bond angle[43] rather than multiple Th–C bonding, the "agostic"[44] nature of the α-hydrogen atom interactions appears again to reflect the pronounced electron deficiency at the d°,f° metal center (F). Similar types of interactions have been recently identified in other organo-f-element compounds.[45]

The molecular structure of **1** reveals a number of H–H nonbonded contacts that are shorter than twice the hydrogen van der Waals radius (1.20–1.45 Å[46]). These include (Figure 6), within the $Th(CH_2CMe_3)_2$ fragment, H_{21B}–H_{35A} = 2.119 Å, H_{11B}–H_{34A} = 2.289 Å, H_{21B}–H_{34A} = 2.478 Å, and from neopentyl-to-Cp′ methyl, H_{21A}–H_{2MB5} = 2.161 Å, H_{11B}–H_{2MB1} = 2.194 Å, H_{21A}–H_{2MB4} = 2.260 Å, and H_{11A}–H_{2MA2} = 2.285 Å. As noted for **3**, it is likely that the configuration of the alkyl groups in the equatorial girdle is strongly influenced by such nonbonded interactions.

The molecular structure of complex **5** has also been determined by single-crystal X-ray diffraction.[29] Although full details are reserved for a later contribution,[29] it is important to note here that the distortion of the $Th(CH_2CMe_3)(CH_2SiMe_3)$ fragment (Figure 3B) is reminiscent of that in **1** and **3**. That the neopentyl ligand exhibits a large Th–C(α)–C(β) angle while the (trimethylsilyl)methyl ligand has a more normal angle is of relevance in discussing sources of regioselectivity (vide infra).

Spectroscopy of $Cp'_2ThR_{2-n}X_n$ Complexes. The unusual distortions observed in **1** (as well as **3**) raise the question of whether unusual spectral parameters are associated with these bonding features and also whether the distorted structures lie in deep potential energy wells. With regard to vibrational spectra, there is no evidence in Nujol mull data for the classic diminution in ν_{C-H} found in many agostic M···H–C interactions.[44] Solution ^1H and ^{13}C NMR spectroscopy of **1** reveals magnetically equivalent neopentyl ligands and neopentyl methyl groups down to −90 °C,[14b] i.e., the distortions clearly do not lie in deep potential energy wells in solution.

To determine whether such distortions have significant spectroscopic consequences in solid-state, high-resolution CP-MAS, ^{13}C NMR[47] studies were conducted for **1**, **3**, **5**, **6**, **8**, and several reference compounds in which distortions were not expected. CP-MAS data and spectral assignments are presented in Table VII. Solution ^{13}C NMR chemical shift and coupling constant data are also tabulated for comparison. Two representative solid-state spectra are reproduced in Figure 7. In all cases, assignment of the ring resonances in the Cp'_2Th fragments is straightforward. Small differences (1–2 ppm) from solution chemical shifts may be due to crystal lattice effects or referencing artifacts. The assignment of the alkyl resonances in the solution spectra follows readily from the chemical shift and $^1J_{C-H}$ data.

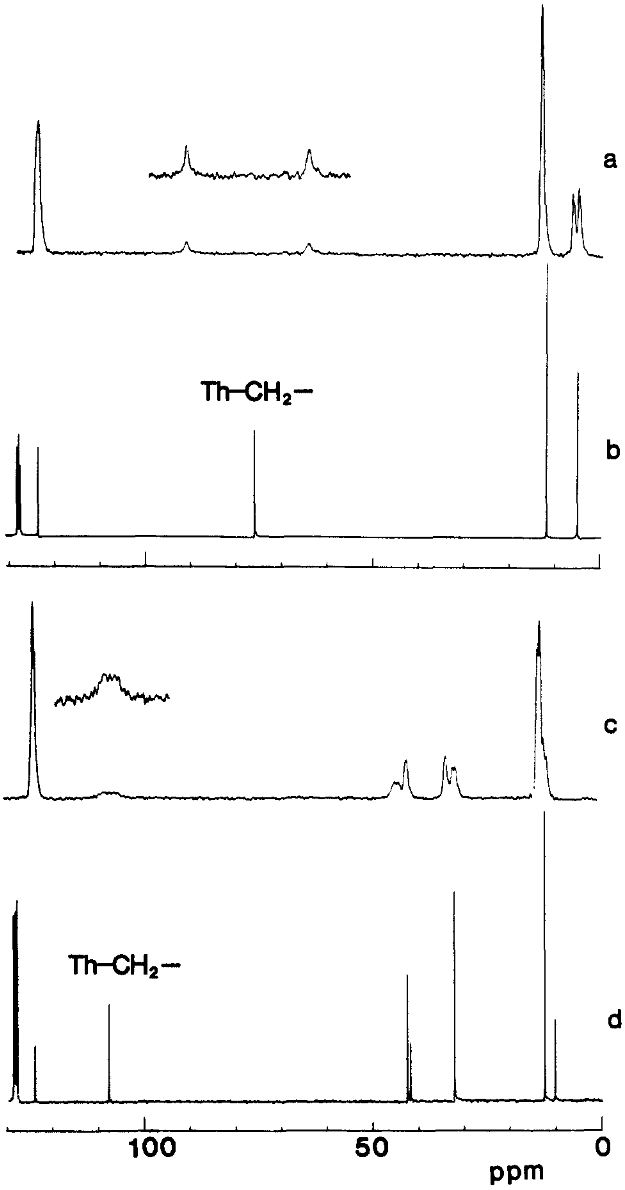

Figure 7. Examples of solid-state ^{13}C CP-MAS NMR spectra compared to solution ^{13}C NMR spectra (a) CP-MAS spectrum of **3**; (b) solution ^{13}C spectrum of **3**; (c) CP-MAS spectrum of **6**; (d) solution ^{13}C spectrum of **6**.

The one-to-one congruence of the solution and solid-state NMR data for Cp'_2ThMe_2 and $Cp'_2Th(CH_2SiMe_3)Cl$ is evident in Table VII. However, the data for compounds **1**, **3**, and **5** evidence pronounced displacements of the $^{13}C(\alpha)$ resonances for the solution positions, consistent with the diffraction-detected distortions. Thus, in solid **3**, the C(α) resonances are split by 27 ppm in an approximately symmetric fashion around the shift position observed in solution. In solid **1**, a signal is observed 12.3-ppm upfield of the solution shift, but no unique methylene signal is detected downfield. However, the Cp′ ring carbons occur precisely where a second C(α) resonance would be expected on the basis of the solution data. Thus, it is likely that this feature is obscured by an accidental degeneracy. The C(α) signals for **5** in the solid state

---

[41] Broach, R. W.; Schultz, A. J.; Williams, J. M.; Brown, G. M.; Manriquez, J. M.; Fagan, P. J.; Marks, T. J. *Science* **1979**, *203*, 172–174.

[42] (a) Churchill, M. R.; Wasserman, H. J. *Inorg. Chem.* **1983**, *22*, 1574–1578. (b) Schultz, A. J.; Brown, R. K.; Williams, J. M.; Schrock, R. R. *J. Am. Chem. Soc.* **1981**, *103*, 169–176. (c) Schrock, R. R. *Acc. Chem. Res.* **1979**, *12*, 98–104. (d) Schultz, A. J.; Williams, J. M.; Schrock, R. R.; Rupprecht, G. A.; Fellmann, J. D. *J. Am. Chem. Soc.* **1979**, *101*, 1593–1595.

[43] Such a description would invoke sp hybridization at C_{1B} to accommodate the large Th–C_{1B}–C_{2B} bond angle and would explain the shortened Th–C_{1B} distance and any shortening of C_{1B}–C_{2B}. The C_{1B}–H_{11B} and C_{1B}–H_{21B} bonds would be largely C_{1B} p in character, explaining the Th–C_{1B}–H bond angles near 90° and the increased C_{1b}–H bond lengths.

[44] Brookhart, M.; Green, M. L. H. *J. Organomet. Chem.* **1983**, *250*, 395–408 and references therein.

[45] (a) Mauermann, H.; Swepston, P. N.; Marks, T. J. *Organometallics* **1985**, *14*, 200–202. (b) Jeske, G.; Schock, L. E.; Swepston, P. N.; Schumann, H.; Marks, T. J. *J. Am. Chem. Soc.*, in press. (c) Tilley, T. D.; Andersen, R. A.; Zalkin, A. *J. Am. Chem. Soc.* **1982**, *104*, 3725–3727.

[46] Huheey, J. E. "Inorganic Chemistry", 3rd ed.; Harper and Row: New York, 1983; pp 258–259.

Table VII. ^{13}C NMR Chemical Shift Data for Cp′$_2$ThR$_2$ Compounds

complex	C(α)	C(β)	C(γ)	C-ring	Me-ring
		Solid (CP–MAS)			
Cp′$_2$ThMe$_2$	68.4	*b*	*b*	123.2	12.2
Cp′$_2$Th(CH$_2$SiMe$_3$)Cl	73.7	*b*	5.5	126.3	12.8
Cp′$_2$Th(CH$_2$CMe$_3$)$_2$ (**1**)	98.5	41.3	38.0	124.7	13.7
Cp′$_2$Th(CH$_2$SiMe$_3$)$_2$ (**3**)	92.0, 65.0	*b*	6.7, 5.4	124.6	13.7
Cp′$_2$Th(CH$_2$CMe$_3$)(CH$_2$SiMe$_3$) (**5**)	95.9	n.o.[c]	37.6	123.5	12.6
	88.5		6.4		
Cp′$_2$Th(CH$_2$CMe$_2$Et)$_2$ (**6**)	108 (br)	41.9	33.3, 31.9	124.1	12.7
			31.2		
Cp′$_2$Th(CH$_2$SiMe$_2$Ph)$_2$ (**8**)	84.6, 62.4	*b*	7.3, 1.2, 0.3	123.6	11.9
		Solution			
Cp′$_2$ThMe$_2$	68.0 (112)[d]	*b*	*b*	122.6	11.0 (126)
Cp′$_2$Th(CH$_2$SiMe$_3$)Cl	71.8 (104)	*b*	4.6 (117)	125.8	11.6 (127)
Cp′$_2$Th(CH$_2$CMe$_3$)$_2$	110.2 (97)	39.1	36.4 (117)	123.7	12.3 (126)
Cp′$_2$Th(CH$_2$SiMe$_3$)$_2$	76.9 (99)	*b*	4.9 (117)	123.7	11.8 (126)
Cp′$_2$Th(CH$_2$CMe$_3$)(CH$_2$SiMe$_3$)	110.7 (100)	39.1	36.6 (122)	123.7	12.1 (126)
	74.2 (11)		4.9 (117)		
Cp′$_2$Th(CH$_2$CMe$_2$Et)$_2$	107.6 (101)	41.7	32.0 (123)	123.8	12.3 (126)
			42.4 (121)		
Cp′$_2$Th(CH$_2$SiMe$_2$Ph)$_2$	73.6 (100)	*b*	3.3 (118)	124.3	11.8 (126)

[a] All chemical shifts are reported in ppm from internal Me$_4$Si. For solution spectra they were measured relative to solvent peaks. For CP–MAS spectra, chemical shifts were measured relative to external hexamethylbenzene. [b] Not present. [c] Not observed. [d] J_{CH} values are reported in Hz in parentheses, all multiplicities are consistent with the assignments.

occur fairly close together, in the region where the upfield C(α) signal of **1** and the downfield signal of **3** appear. With the structural results for **5** (Figure 3B) in hand, it is possible to completely assign the CP–MAS spectrum. For all but the α-carbons of the branched alkyl group, the assignment is trivial and is based upon chemical shifts and multiplicities observed in coupled solution spectra. By comparison with the solid-state spectra of **1** and **3** it is clear that the CP–MAS C(α) resonances for **5** correspond to the downfield resonance of a CH$_2$SiMe$_3$ ligand and the upfield shift of a CH$_2$CMe$_3$ ligand. Since the structural results indicate that the CH$_2$SiMe$_3$ ligand in **5** is distorted, the downfield methylene resonances in the spectra of **1** and **3** must be due to the distorted ligand and the upfield resonance due to the "normal" ligand.

It is interesting to note that the solid-state NMR spectra of **6** and **8** do not evidence the dispersion in C(α) chemical shifts observed in **1**, **3**, and **5**. This result implies that either interconversion of C(α) environments is rapid on the NMR time scale in the solid at room temperature or that the degree of distortion is less in these compounds.

Discussion

Since our initial discovery of the actinide-centered cyclometalation processes **1** → **2** and **3** → **4**, we have scrutinized the chemical, thermochemical, kinetic/mechanistic, and structural aspects of these and related transformations in some detail. Such reactions offer an ideal opportunity to understand intramolecular (and intermolecular[7g,h,12]) C–H activation patterns involving saturated hydrocarbon fragments and metal centers incapable of supporting classical oxidative addition–reductive elimination sequences. The thermochemical studies, which have been reported already,[15] indicate that processes such as **1** → **2** are actually endothermic, with the exact ΔH for the process reflecting a balance between opposing destabilization of the starting dialkyl (evident in the highly distorted structures of **1**, **3**, and **5**) and ring strain in the product metallocycle (~16 kcal mol^{-1} in **2**, ~8 kcal mol^{-1} in **4**). It is concluded that, in a closed container,[48] the reaction is entropically driven with a reasonable estimate[3,8] of the $T\Delta S$ contribution to ΔG (rotational and translational for one particle → two particles) being ca. 10–12 kcal mol^{-1} ($\Delta S \sim +$ 30–35 eu) under typical cyclometalation conditions. The focus of the present discussion is to integrate this information with the mechanistic, structural, and regiochemical results that have now emerged.

Cyclometalation Mechanism. Scheme V shows what we believe to be the five most plausible pathways for actinide-centered cyclometalation; each has some precedent. Mechanism E is analogous to known platinum metal chemistry (Scheme I),[2,3,4] but appears highly unlikely in view of the inaccessibility of the Th(VI) formal oxidation state.[37] A homolytic free radical or solvent-mediated process such as D can be discounted as a significant pathway since no deuterium is incorporated in the volatiles when thermolysis is carried out in deuterated solvents. Pathway C is an α-hydrogen atom activation process, which is common in high-valent group 5 as well as other f-element and early transition-metal chemistry.[42c,49] In the present case, it can be ruled out as a major pathway on the basis of experiments with deuterium-labeled α-carbon atoms (**11** and **12** in Scheme IV). The merits of pathway A vs. B can be tested by labeling the protons in the γ-methyl groups of an appropriate cyclometalation precursor and determining whether the label is transferred to the volatile product. For this purpose, compound **13** was chosen since it can be readily prepared in large quantities and because all aspects of the **3** → **4** thermolysis chemistry appear to be representative of this class of cyclometalation reactions.

Interestingly, the volatiles from thermolysis of **13** in C$_6$D$_{12}$ were found to contain *both* Me$_4$Si-d_9 and Me$_4$Si-d_{10} in a ratio which depends upon the reaction temperature (Table II and Scheme IV). The possible sources of H atoms in this experiment are Cp′ methyl groups and α-CH$_2$ functionalities; as already noted, the latter source can be ruled out on the basis of labeling experiments (vide supra). There is, of course, considerable precedent for hydrogen atom abstraction processes involving Cp′ ligands.[7g,12,32b,49c,d,50] However, the crucial question in the present context is what role Cp′ and γ-hydrogen activation play in the reaction **3** → **4** (and pathways I and II in Scheme IV). In the discussion which follows, it is argued that the mechanistic data are most consistent with a scenario in which the processes represented as A and B in Scheme V represent competing routes from **3** to **4** (processes I

---

(47) (a) Fyfe, C. A. "Solid State NMR for Chemists"; CFC Press: Guelph, 1985. (b) Maciel, G. D. *Science* **1984**, *226*, 282–288. (c) Wasylishen, R. E.; Eyre, C. A. *Ann. Repts. NMR Spectros.* **1982**, *12*, 1–80. (d) Yannoni, C. S. *Acc. Chem. Res.* **1982**, *15*, 201–206.

(48) An approximate Raoult's law calculation for neopentane in cyclohexane (assuming $\Delta H_{mixing} \sim 0$) indicates that for a typical **1** → **2** thermolysis in a sealed NMR tube or closed reaction vessel, greater than ca. 97% of the neopentane will be in the solution phase. Thus, for this system, where the organic cyclometalation product is the most volatile, escape of neopentane from the solution should have only a minor effect on the position of the cyclometalation equilibrium.

(49) (a) Chamberlain, L. R.; Rothwell, A. P.; Rothwell, I. P. *J. Am. Chem. Soc.* **1984**, *106*, 1847–1848. (b) Chamberlain, L.; Rothwell, I. P.; Huffman, J. C. *J. Am. Chem. Soc.* **1982**, *104*, 7338–7340. (c) He, M.-Y.; Xiong, G.; Toscano, P. J.; Burwell, R. L., Jr.; Marks, T. J. *J. Am. Chem. Soc.* **1985**, *107*, 641–652. (d) He, M.-Y.; Burwell, R. L., Jr.; Marks, T. J. *Organometallics* **1983**, *2*, 566–569.

and II in Scheme IV) and that pathway B is only important in the thermolysis of **13** (not **3**), where a large kinetic isotope effect is operative.

That the cyclometalation of **3** (and **13**) can be described by pathways A and B (and only A and B) as drawn is supported by a number of lines of evidence. First, the clean nature of the reactions as monitored by 270-MHz ^{1}H NMR spectroscopy argues that no intermediate species build up during the reaction and that the metallacycles are the only significant organometallic products. That both A and B are indeed unimolecular reactions is supported by the well-behaved first-order kinetics observed and that the ratio of product isotopomers is independent of reactant concentration and solvent identity. Further support for our contention that Me_4Si-d_9 arises from mechanism B, which involves intramolecular opening of a ring-metalated ($Th[\eta^6$-$(CH_3)_4C_5CH_2]$) intermediate, is provided by the deuterium balance: the Me_4Si-d_9 yield correctly correlates with the observed yield of $Cp'H$-d_1 (obtained by hydrolysis of the cyclometalation product). That the rate-limiting step in mechanism B is ring attack is supported by the observation that the only deuterated CpH′ species observed is $Cp'H$-d_1. If the first step were reversible and the opening of the ring-metalated species were rate-determining, multiply deuterated Cp′H products would be expected.[35]

In addition to the above evidence, the rate and activation parameter data (Scheme IV) suggest that while the Me_4Si-d_{10} arises via a process similar in nature to the other γ-hydrogen cyclometalations (especially $\mathbf{3} \rightarrow \mathbf{4}$), the Me_4Si-d_9 arises from a different type of transition state (the disparity in $\Delta S^\ddagger$ is particularly evident). From these results, we associate process I with the normal cyclometalation pathway, A, and process II with the ring activation pathway, B. From the data in Table I it can be seen that process II is ca. 20 times slower than $\mathbf{3} \rightarrow \mathbf{4}$. If it is reasonably assumed that there is only a minor γ-secondary kinetic isotope effect for process II, then cyclometalation via mechanism A (corresponding to process I) should dominate (>95%) the thermolysis chemistry of compound **3**. The kinetic isotope effect for process I is found to be 10.0 (5) at 85 °C and 8.5 (5) at 115 °C. Such a result implies significant C–H bond scission in the rate-determining step; the magnitude of k_H/k_D has precedent in other types of C–H abstraction processes.[12,51-53]

Structural Considerations. The neutron-diffraction-derived molecular structure of **1** provides the most detailed view to date of the ligand disposition in a thorium dialkyl which undergoes cyclometalation to a thoracyclobutane. As in the structures of **5**, **3**, and $Me_2Si[(CH_3)_4C_5]_2Th(CH_2SiMe_3)_2$,[54] the alkyl ligation is very unsymmetrical (cf., D), with one highly distorted Th–alkyl linkage and a rather close, interligand $C(\alpha)$–$C(\gamma)$ contact. With regard to the cyclometalation mechanism, a tempting hypothesis might be that such structures represent a ground state that is not distant from the transition state proposed for pathway A. This hypothesis would suggest that the distorted ligand is being moved aside by incipient interactions involving the thorium, a γ-methyl hydrogen of the normal alkyl ligand, and the $C(\alpha)$ of the distorted ligand. In effect, the distorted ligand would be in the process of departing.

Although pathway A may indeed portray a viable description of the cyclometalation reaction coordinate, any *verbatim* mechanistic correlation with the solid-state structural data appears to be only superficial. Thus, the Th–C distances involving the distorted ligand are invariably *shorter* than normal Th–C distances. Second, the solid-state structure of **5**, having Th–CH_2SiMe_3 as the distorted ligand, would in this hypothesis predict cyclometalation to **2** rather than **4**, which is the observed product.[55] Third, the positions of H_{11B}, H_{21B}, and H_{34A} or H_{15A} in **1** indicate that in this particular conformation, C_{1B} is not readily open to receive a hydrogen atom from the other neopentyl ligand. Finally, the solid-state and solution NMR data indicate that while the electronic consequences of the alkyl ligand distortions are by no means insignificant, these distortions do not lie in deep potential energy wells, i.e., in solution, the molecules are not rigidly locked in the observed solid-state conformations.

The highly unsymmetrical nature of the alkyl ligation in **1**, **3**, **5**, and $Me_2Si[(CH_3)_4C_5]_2Th(CH_2SiMe_3)_2$ appears to arise from a combination of steric and electronic factors (the former appears to be highly dominant). Although many aspects of the distorted alkyl group coordination are reminiscent of alkyldiene-like coordination (E, F) and analogous types of α-hydrogen atom "agostic" interactions have been identified in other electron-deficient f-element organometallics,[45] the present neutron-diffraction results on **1** also underscore the severity of the Cp′–alkyl, interalkyl, and intraalkyl nonbonded interactions. Reference to Figure 6 reveals a number of Cp′–alkyl interactions which are likely to increase the Th–C_{1B}–C_{2B} angle. Such a distortion and concomitant partial rehybridization from $sp^3 \rightarrow sp$ at C_{1B} rationalize many of the observed structural features.

Regioselectivity. A particularly intriguing aspect of the present cyclometalation chemistry is the high selectivity with which the various metallacycles are formed. The reason for this appears to reflect a blend of bond strength/thermodynamic and steric/reactivity factors. In all cases, the regioselectivity appears to be consistent with the rather negative entropies of activation, which suggest highly ordered transition states, i.e., transition states in which there has been substantial loss in internal rotational degrees of freedom, and with rate-limiting C–H bond scission. Some aspects of this chemistry are reminiscent of Thorpe–Ingold-type kinetic and thermodynamic substituent effects, which are common in many cyclization reactions.[8b] The absence of a stable metallacyclic product in the thermolysis of $Cp'_2Th(CH_2CH_2CH_3)_2$ could be taken as further evidence, although all details of the thermolysis mechanism have not been elucidated.

In the case of the $\mathbf{5} \rightarrow \mathbf{4}$ cyclometalation, the reaction pathway involves the cleavage of the weaker thorium-to-carbon bond (D(Th–CH_2CMe_3) ~ 72 kcal mol^{-1} vs. D(Th–CH_2SiMe_3) ~ 80 kcal mol^{-1}) to yield the enthalpically favored (less strained)[16] product ($\mathbf{5} \rightarrow \mathbf{2}$ is more endothermic by ca. 28 kcal mol^{-1}). Interestingly, the activation parameters are closer to those of $\mathbf{1} \rightarrow \mathbf{2}$, where a Th–CH_2CMe_3 bond is also broken, than to $\mathbf{3} \rightarrow \mathbf{4}$, where a Th–CH_2SiMe_3 bond is broken.[56] Although these results are consistent with significant thermodynamic control, it should also be noted that a C–H bond on an Si–CH_3 functionality is likely to be more reactive than that on a C–CH_3 functionality.[57]

The selective formation of a 4-membered ring in the $\mathbf{6} \rightarrow \mathbf{7}$ cyclometalation at first appears surprising in view of platinum-

---

(50) (a) McDade, C.; Green, J. C.; Bercaw, J. E. *Organometallics* **1982**, *1*, 1629–1634 and references therein. (b) Watson, P. L. *J. Chem. Soc., Chem. Commun.* **1983**, 276–277. (c) Bulls, A. R.; Bercaw, J. E., Abstracts, 190th ACS National Meeting, Chicago, IL; Sept. 8–13, 1985; INOR 131. (d) Marks, T. J., lecture presented at the 190th ACS National Meeting, Chicago, IL; Sept. 8–13, 1985; INOR 251 (crystal structure of $Cp'Zr[\eta^6$-$(CH_3)_4C_5CH_2]C_6H_5)$. (e) Schock, L. E.; Brock, C. P.; Marks, T. J., submitted for publication.

(51) Mayer, J. M.; Curtis, C. J.; Bercaw, J. G. *J. Am. Chem. Soc.* **1983**, *105*, 2651–2660.

(52) (a) Marks, T. J. *Acc. Chem. Res.* **1976**, *9*, 223–230 (Cp_3UR thermolysis). (b) Marks, T. J.; Seyam, A. M.; Kolb, J. R. *J. Am. Chem. Soc.* **1973**, *95*, 5529–5539.

(53) (a) Carpenter, B. K. "Determination of Organic Reaction Mechanisms"; John Wiley: New York, 1984; Chapter 5 and references therein. (b) More O'Ferrall, R. A. In "Proton-Transfer Reactions"; Caldin, E., Gold, V., Eds.; Chapman and Hall: London, 1975; Chapter 8. (c) Buddenbaum, W. E.; Shiner, V. J., Jr. In "Isotope Effects on Enzyme-Catalyzed Reactions"; Cleland, W. W., O'Leary, M. H., Northrop, D. B., Eds.; University Park Press: Baltimore, 1977; pp 1–36. (d) Wolfsberg, M. *Acc. Chem. Res.* **1972**, *5*, 225–233.

(54) (a) Fendrick, C. M.; Mintz, E. A.; Schertz, L. D.; Marks, T. J.; Day, V. W. *Organometallics* **1984**, *3*, 819–821. (b) Although it might appear a priori, that "pulling back" of the Cp'_2 ligation in this compound might alleviate Cp′–alkyl nonbonded repulsions, a detailed analysis of the nonbonding contacts reveals a situation rather similar to that in **3** (Smith, G. M.; Marks, T. J., unpublished results).

(55) It is unlikely that **2** can be an intermediate alongthe $\mathbf{5} \rightarrow \mathbf{4}$ pathway, since **2** (but not **4**) would be rapidly converted to $Cp'_2Th(C_6H_5)_2$ when the reaction was carried out in benzene.[14a] The diphenyl product is not observed.

(56) Some of the $\Delta S^\ddagger$ for $\mathbf{5} \rightarrow \mathbf{4}$ presumably reflects the additional entropic cost of selecting between the two alkyl ligands.

(57) (a) Armitage, D. A. In ref 37b, Chapter 9.1, pp 8–10. (b) Farah, D.; Karol, T. J.; Kuivlia, H. G. *Organometallics* **1985**, *4*, 662–666 and references therein.

contered processes[3] where, in the most closely analogous case, a metallacyclopentane is formed exclusively (eq 13) or where, in other cases, little or no cyclometalation selectivity is observed

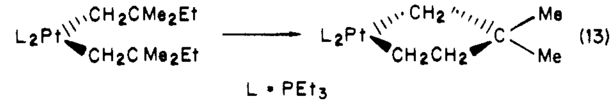

(mixtures of 4-, 5-, and 6-membered rings are obtained). However, C–H activation appears not to be rate-determining in the platinum chemistry (cf., Scheme I), and these selectivity results have thus been taken as evidence for approximately equal strain energies in the various platinacycles. The **6** → **7** reaction differs in that C–H scission is now rate-determining, so that **7** may be a kinetic rather than a thermodynamic product. However, that the ring strain in **4** is ca. 8 kcal mol^{-1} less than that in **2** suggests, for $Cp'_2Th<$ systems, that the strain energy is rather sensitive to the metallacycle constituents and that the metallacyclopentane may well be less strained than the metallacyclobutane. Thus, it appears that the thorium-centered reaction discriminates kinetically between the C–H bonds of the neohexyl methyl and ethyl groups. The most likely reason is the substantial congestion about the reaction center. The activation parameters of Scheme II support this argument in that greater steric crowding imparted by adding an ethyl group should destabilize the ground state (lower ΔH^{*}) and require greater selectivity in the transition state (more negative ΔS^{*}). Such phenomenology is, to some extent, suggestive of classical Thorpe–Ingold effects.[8b] Efforts to determine whether **7** could be isomerized thermally to a thoracyclopentane were frustrated by decomposition to a variety of nonmetallacyclic, unidentified products.

The cyclometalation of **8** to form **9**, followed by the isomerization of **9** to **10**, provides additional evidence that thoracyclobutanes can be produced under kinetic control. This result demonstrates that the reaction environment is sufficiently selective not only to discriminate between methyl and ethyl groups but also to exclude an inherently more reactive aryl C–H functionality on a bulky group in favor of a more accessible, presumably less reactive methyl C–H functionality. In comparing the activation parameters of **8** → **9** to **3** → **4**, an obvious analogy to the **6** → **7**/**1**→ **2** pair is evident: decreased ΔH^{*}, presumably due to crowding, and more negative ΔS^{*}, presumably due to the higher selectivity exercised.

The isomerization of **9** → **10** demonstrates that the thoracyclobutane is a kinetic product and that subsequent rearrangement to **10** represents ultimate thermodynamic control. Since a $Th-C_6H_5$ bond disruption enthalpy is ca. 9 kcal mol^{-1} greater than that of a $Th-CH_2SiMe_3$ bond,[15,58] it is not possible to identify the release of ring strain as the driving force for **8** → **9**. As to the mechanism, it appears unlikely that direct metalation of the aryl C–H bond by the metallacycle $Th-CH_2Si$ bond is geometrically feasible. The intermediacy of ring-metalated species appears more likely. Such a mechanism could in principle be tested by tracing the course of deuterium labels in the thermolysis of $Cp'_2Th[CH_2SiMe(C_6D_5)CH_2]$, prepared in turn from $Cp'_2Th(CH_2SiMe_2C_6D_5)_2$.

Conclusions

The results of this study provide the most complete description to date of thorium-centered cyclometalation processes which effect intramolecular C–H functionalization of saturated hydrocarbon ligands. The unimolecular kinetics, regioselectivity for kinetic products, congested ground-state structures, rate-limiting C–H bond scission, large negative entropies of activation, and the apparent absence of a high-energy, thorium-centered HOMO,[59,60] implicate a highly organized, sterically constrained, electrophilic transition state for cyclometalation. A "heterolytic" "four-center" transition state such as G appears reasonable for such a process

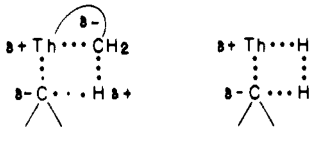

G H

and bears close analogy to transition states previously proposed[19] for actinide-centered H_2 activation (H). In sharp contrast, cyclometalation processes involving more electron-rich middle and late transition metals frequently involve ligand dissociation or reductive elimination of a multiatom fragment (creating a sterically and electronically unsaturated metal center) prior to C–H activation by oxidative addition. The C–H bond activation process is usually not rate-limiting; in many cases it apparently occurs with a low activation energy and is not highly selective.[3-7]

Several aspects of the Cp'_2ThR_2 cyclometalation process merit additional comment. While rather large, negative entropies of activation observed ($\Delta S^{*} \sim -15$ to -20 eu) may be a characteristic of such reactions, they were unexpected at the outset of this study. Such ΔS^{*} values are not totally unprecedented for intramolecular rearrangements;[61] however, they appear to be rather unusual for processes in which a fragment is expelled ($\Delta S \sim +30$ eu for the present reactions).[61] More relevant to C–H bond activation problems, the large, negative ΔS^{*} values raise the possibility that intramolecular activation processes will not always enjoy an entropically-based kinetic advantage[6] over intermolecular ones.[7e] Indeed, it can be asked why the present Cp'_2ThR_2 systems do not undergo intermolecular C–H activating reactions and under what conditions might such processes occur to the exclusion of cyclometalation.

With regard to saturated hydrocarbon activation, none of the Cp'_2ThR_2 cyclometalation precursors have been observed to undergo significant reaction with protiated aliphatic (noncyclic) hydrocarbon solvents.[62] Much of the reason may be steric, since molecules such as $Cp'_2Th(CH_2CMe_3)_2$ are highly crowded (cf., Figures 5 and 6), and the approach of an alkane substrate molecule toward the Th–C σ bonds in the "equatorial girdle" will be severely impeded by nonbonded interactions with Cp′ and alkyl ligand hydrogen atoms. What about more reactive solvents? The best characterized system to date is $Cp'_2Th(CH_2CMe_3)_2 + C_6H_6/C_6D_6$.[14a,19,32,63] At 70 °C, the reaction of **1** with neat C_6D_6 takes place only (≥97%) via **2** (eq 14), as monitored by ^1H NMR (the

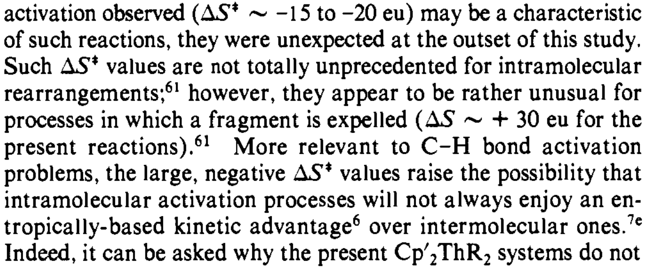

signals for complex **2** behave as expected for an intermediate in a two-step, consecutive process) and deuterium labels. At 70 °C in neat C_6D_6, the cyclometalation proceeds with a first-order rate constant $k = 7.30\ (12) \times 10^{-5}\ s^{-1}$ while the reaction of **2**[12] with neat C_6D_6 proceeds with a pseudo-first-order rate constant $k = 7.0\ (2) \times 10^{-5}\ s^{-1}$.[19,32,63] Again, the intermolecular **1** + benzene

---

[58] Sonnenberger, D. C.; Morss, L. R.; Marks, T. J. *Organometallics* **1985**, *4*, 352–355.

[59] (a) Ciliberto, C.: Condorelli, G.; Fagan, P. J.; Manruquez, J. M.; Fragalâ, I.; Marks, T. J. *J. Am. Chem. Soc.* **1981**, *103*, 4755–4759 and references therein. (b) Fragalā, I.; Gulino, A. In ref 37a, pp 327–360. (c) Bursten, B. E.; Fang, A. *J. Am. Chem. Soc.* **1983**, *105*, 6495–6496.

[60] For coordinatively unsaturated d^8 complexes, a high-lying, metal-centered HOMO appears to be a necessary condition for C–H activation via oxidative addition.[6d]

[61] See, for example: (a) ref 53a, Chapter 7. (b) Harris, J. M.; Wamser, C. C. "Fundamentals of Organic Reaction Mechanisms"; Wiley: New York, 1976; pp 108–110.

[62] By virtue of steric bulk, the "weak" secondary Th–C σ bond that would form[58] and the expected kinetic isotope effect for C–H activation, the low reactivity of C_6D_{12}[12] is understandable.

[63] (a) $k_{C_6H_6}/k_{C_6D_6} \approx 1.5$. (b) Assuming velocity = $k_2[\mathbf{2}][C_6D_6]$, $k_2 \sim 6.2 \times 10^{-6}\ M^{-1}\ s^{-1}$. (c) From mechanistic studies of other **2** + RH systems,[12] it is likely that thoracyclobutane ring-opening is stepwise. For **2** + Me_4Si, velocity = $k[\mathbf{2}][Me_4Si]$.

process is not competitive with cyclometalation, and in this case there is no doubt that the intermolecular reaction product is thermodynamically favored ($\Delta H_{calcd} \sim -19$ kcal mol^{-1}).[15]

On a more general level, the present observations regarding the rather stringent spatial requirements of transition states such as G suggest that four-center, heterolytic types of processes offer a means to effect homogeneous C–H activation on saturated hydrocarbons with high intrinsic regioselectivity. Such an approach is presently under investigation.

Acknowledgment. We thank the National Science Foundation for support of this research at Northwestern University under grant CHE83-06255 and the Office of Basic Energy Sciences, Division of Materials Science, U.S. Department of Energy, for support of the neutron diffraction work at Argonne National Laboratory under contract W-31-109-Eng-38. We thank Dr. Paul Toscano for assistance in obtaining CP-MAS NMR spectra, Professor Victor Day for helpful discussions, and Dr. Doris Hung for GC-MS data.

Supplementary Material Available: A table of general temperature factor expressions (Table V) as well as a listing of observed and calculated structure factors from the final cycle of least-squares refinement for $Cp'_2Th(CH_2CMe_3)_2$; ^1H NMR spectra recorded during the course of the **6** → **7** thermolysis reaction (Figure S-1) and during the course of the **7** + Me_4Si reaction (Figure S-2) (20 pages). Ordering information is given on any current masthead page.

A Synthetic and Mechanistic Study of Oxycarbene-like Coupling Reaction Patterns of Actinide η^2-Acyl Complexes with Carbon Monoxide and Isocyanides

Kenneth G. Moloy, Paul J. Fagan, Juan M. Manriquez, and Tobin J. Marks*

Contribution from the Department of Chemistry, Northwestern University, Evanston, Illinois 60201.

Received May 13, 1985

Abstract: This contribution reports the synthesis and characterization of the ylide complexes $Cp'_2Th[OC(CH_2\text{-}t\text{-}Bu)C(PR_3)O](Cl)$ ($Cp' = \eta^5\text{-}C_5Me_5$; R = Me, Ph) formed by the carbonylation of $Cp'_2Th(Cl)(\eta^2\text{-}COCH_2\text{-}t\text{-}Bu)$ (**1**) in the presence of phosphines. Isotopic tracer studies with ^{13}CO indicate that the labeled carbon atom is incorporated regiospecifically at the ylide α-carbon atom position. The carbonylation of **1** to yield the enedionediolate $\{Cp'_2Th[OC(CH_2\text{-}t\text{-}Bu)CO](Cl)\}_2$ (**2**) or the ylide complexes was found to obey a second-order rate law where rate = $kP_{CO}[\mathbf{1}]$; $k = 1.50\ (5) \times 10^{-5}$ min^{-1} torr^{-1} for both carbonylations at 30.8 °C. The rate of formation of the ylide complexes was also found to be independent of solvent, phosphine concentration, and type of phosphine used. The carbonylation of **1** is therefore inferred to involve a rate-determining coupling of CO with the acyl to yield an intermediate ketene or ketene-like complex. The reaction of acyl **1** or $Cp'_2Th(Cl)(\eta^2\text{-}COCH_2Ph)$ with a variety of isocyanides (RNC; R = *t*-Bu, C_6H_{11}, 2,6-$Me_2C_6H_3$) results in the formation of ketenimine complexes of the type $Cp'_2Th[OC(CH_2\text{-}t\text{-}Bu)CNR](Cl)$ and $Cp'_2Th[OC(CH_2Ph)CNR](Cl)$. Addition of a second equivalent of isocyanide yields simple adducts of the type $Cp'_2Th[OC(CH_2\text{-}t\text{-}Bu)CNR](CNR)(Cl)$ and $Cp'_2Th[OC(CH_2Ph)CNR](CNR)(Cl)$. These new complexes have been fully characterized by standard techniques and the ketenimine $Cp'_2Th(Cl)[OC(CH_2\text{-}t\text{-}Bu)(CN\text{-}2,6\text{-}Me_2C_6H_3)]$ by single-crystal X-ray diffraction. Under the appropriate conditions, the *N*-aryl complexes suffer secondary reactions in which the η^2-acyl ultimately undergoes coupling with 2 equiv of isocyanide to yield acetylindolate and acetylindoleninate derivatives. The η^2-acyl was also found to undergo coupling with 1 equiv of diphenylketene to yield the complex $Cp'_2Th[OC(CH_2\text{-}t\text{-}Bu)C(CPh_2)O](Cl)$. These coupling products have been fully characterized by conventional analytical and structural methodology. The mechanistic and reactivity results of this study are discussed in terms of the anchored Fischer carbene-like character of actinide η^2-acyls and the mechanism by which the carbonylation of **1** yields the enedionediolate **2**.

The bonding and reactivity properties of actinide,[1] lanthanide,[1a,2] and early transition element[1e,3-6] acyl complexes have recently been the subject of considerable attention. In particular, many of the spectroscopic, structural, and reactivity characteristics of these η^2-acyls are distinctive vis-à-vis those of middle and late transition elements and evidence unusual, perhaps catalytically significant,[1,7] modes of CO activation. To the extent that most metal–ligand bonding/reactivity descriptions are based upon formalisms and

---

(1) (a) Marks, T. J.; Day, V. W. In "Fundamental and Technological Aspects of Organo-f-Element Chemistry"; Marks, T. J., Fragalà, I. L., Eds.; Reidel: Dordrecht, 1985; pp 115–157. (b) Marks, T. J.; Ernst, R. D. In "Comprehensive Organometallic Chemistry"; Wilkinson, G. W., Stone, F. G. A., Abel, E. W., Eds.; Pergamon Press: Oxford, 1982, Chapter 21. (c) Marks, T. J. *Science* **1982**, *217*, 989–997. (d) Fagan, P. J.; Maatta, E. A.; Marks, T. J. *ACS Symp. Ser.* **1981**, *152*, 53–78. (e) Fagan, P. J.; Manriquez, J. M.; Marks, T. J.; Day, V. W.; Vollmer, S. H.; Day, C. S. *J. Am. Chem. Soc.* **1980**, *102*, 5393–5396.

(2) (a) Evans, W. J.; Wayda, A. L.; Hunter, W. E.; Atwood, J. L. *J. Chem. Soc., Chem. Commun.* **1981**, 706–708. (b) Evans, W. J. *Adv. Organomet. Chem.* **1985**, *24*, 131–177.

(3) (a) Wolczanski, P. T.; Bercaw, J. E. *Acc. Chem. Res.* **1980**, *13*, 121–127 and references therein. (b) Lappert, M. F.; Juong-Thi, N. T.; Milne, C. R. C. *J. Organomet. Chem.* **1979**, *74*, C35–C37. (c) Teuben, J. H., in ref 1a, pp 195–227.

(4) (a) Calderazzo, F. *Angew. Chem., Int. Ed. Engl.* **1977**, *16*, 299–311. (b) Fachinetti, G.; Floriani, C.; Roselli, A.; Pucci, S. *J. Chem. Soc., Chem. Commun.* **1978**, 269–270. (c) Fachinetti, G.; Floriani, C.; Stoeckli-Evans, H. *J. Chem. Soc., Dalton Trans.* **1977**, 2297–2302. (d) Fachinetti, G.; Fochi, G.; Floriani, C. *J. Chem. Soc., Dalton Trans.* **1977**, 1946–1950. (e) Fachinetti, G.; Floriani, C. *J. Organomet. Chem.* **1974**, *71*, C5–C7.

(5) (a) Kropp, K.; Skibbe, V.; Erker, G.; Kruger, C. *J. Am. Chem. Soc.* **1983**, *105*, 3353–354. (b) Erker, G.; Kropp, K. *Chem. Ber.* **1982**, *115*, 2437–2446. (c) Erker, G.; Kropp, K.; Kruger, C.; Chiang, A.-P. *Chem. Ber.* **1982**, *115*, 2447–2460. (d) Erker, G. *Acc. Chem. Res.* **1984**, *17*, 103–109.

(6) (a) Kreissl, F. R.; Sieber, W. J.; Wolfgruber, M.; Reide, J. *Angew. Chem., Int. Ed. Engl.* **1984**, *23*, 640. (b) Curtis, M. D.; Shiu, K.-B.; Butler, W. M. *Organometallics* **1983**, *2*, 1475–1477. (c) Roper, W. R.; Taylor, G. E.; Waters, J. M.; Wright, L. J. *J. Organomet. Chem.* **1979**, *182*, C46–C48. (d) Franke, U.; Weiss, E. *J. Organomet. Chem.* **1979**, *165*, 329–340. (e) Carmona-Guzman, E.; Wilkinson, G.; Atwood, J. L.; Rogers, R. D.; Hunter, W. E.; Zaworotko, M. J. *J. Am. Chem. Soc., Chem. Commun.* **1978**, 465–466.

(7) (a) Moloy, K. G.; Marks, T. J. *J. Am. Chem. Soc.* **1984**, *106*, 7051–7064. (b) Maatta, E. A.; Marks, T. J. *J. Am. Chem. Soc.* **1981**, *103*, 3576–3578. (c) Katahira, D. A.; Moloy, K. G.; Marks, T. J. *Organometallics* **1982**, *1*, 1723–1726. (d) Freudenberger, J. H.; Orchin, M. *Organometallics* **1982**, *1*, 1408–1410. (e) Flood, T. C. *Top. Stereochem.* **1981**, *12*, 37–79 and references therein.

0002-7863/86/1508-0056$01.50/0